AWARD NUMBER: W81XWH-16-2-0051

TITLE: Novel Therapeutic Small-Molecule Strategy Targeting Bone Morphogenetic Protein Signaling to Prevent Upper Extremity Heterotopic Ossification

PRINCIPAL INVESTIGATOR: Benjamin Levi, MD

CONTRACTING ORGANIZATION: Regents of the University of Michigan

REPORT DATE: Dec 2019

TYPE OF REPORT: Final Report

PREPARED FOR: U.S. Army Medical Research and Materiel Command
Fort Detrick, Maryland 21702-5012

REPORT DOCUMENTATION PAGE

Form Approved
OMB No. 0704-0188

1. REPORT DATE	2. REPORT TYPE	3. DATES COVERED
Dec 2019	Final	09/30/2016 - 09/29/2019

4. TITLE AND SUBTITLE
Novel Therapeutic Small-Molecule Strategy Targeting Bone Morphogenetic Protein Signaling to Prevent Upper Extremity Heterotopic Ossification

5a. CONTRACT NUMBER

5b. GRANT NUMBER
W81XWH-16-2-0051

5c. PROGRAM ELEMENT NUMBER

6. AUTHOR(S)
Benjamin Levi

E-Mail: blevi@umich.edu

5d. PROJECT NUMBER

5e. TASK NUMBER

5f. WORK UNIT NUMBER

7. PERFORMING ORGANIZATION NAME(S) AND ADDRESS(ES)
Reagents of the University of Michigan
Kathryn Dewitt
503 Thompson St
Ann Arbor MI 48109-1340

8. PERFORMING ORGANIZATION REPORT NUMBER

9. SPONSORING / MONITORING AGENCY NAME(S) AND ADDRESS(ES)
U.S. Army Medical Research and Materiel Command
Fort Detrick, Maryland 21702-5012

10. SPONSOR/MONITOR'S ACRONYM(S)

11. SPONSOR/MONITOR'S REPORT NUMBER(S)

12. DISTRIBUTION / AVAILABILITY STATEMENT
Approved for Public Release; Distribution Unlimited

13. SUPPLEMENTARY NOTES

14. ABSTRACT Over 60% of wounded warriors injured by explosive devices or burns will develop heterotopic ossification (HO), the pathologic formation of mature bone in soft tissues such as muscle, tendon, or even joint spaces. HO presents a significant barrier to quality of life, by delaying rehabilitation and causing chronic pain, open wounds, and joint immobility and contractures. Patients with traumatic burn injuries are at particular risk of developing upper extremity HO severely limiting their functional and vocational abilities. Patients who present with radiographic evidence of HO often undergo surgical excision, which yields dissatisfying results due to incomplete resection, a high risk of recurrence, and an inability to restore range of motion, or improve chronic pain. Drugs which exist can cause adverse healing effects in trauma patients, require long-term treatment, and are unable to be implemented in patients with the highest risk only. Thus, a need exists to prevent HO using therapeutics and minimize treatment duration to avoid adverse effects. The central goal of this grant was to inhibit the non-canonical (TAK1) and canonical (ALK2) bone morphogenetic (BMP) signaling pathways, two synergistic pathways critical for mesenchymal condensation and cartilage formation to prevent or eliminate HO and mitigate joint contractures. We demonstrated the ability of these therapeutics to mitigate HO in our proven animal trauma models. Our overall goal was to generate a paradigm shift in our approach to patients at risk for HO, from delayed surgical excision or long-term treatment with non-specific inhibitors, to early preventative strategies which target high risk individuals with synergistic therapeutics. Having validated the efficacy of these treatments in animal models and cell lines, we believe the next step is to translate these to clinical studies.

15. SUBJECT TERMS
Heterotopic Ossification, Tak1, Alk2, BMP, near-infrared imaging

16. SECURITY CLASSIFICATION OF:			17. LIMITATION OF ABSTRACT	18. NUMBER OF PAGES	19a. NAME OF RESPONSIBLE PERSON
a. REPORT	b. ABSTRACT	c. THIS PAGE			USAMRMC
Unclassified	Unclassified	Unclassified	Unclassified		19b. TELEPHONE NUMBER *(include area code)*

TABLE OF CONTENTS

1. **INTRODUCTION:** Narrative that briefly (one paragraph) describes the subject, purpose and scope of the research.

Over 60% of those wounded warriors injured by explosive devices or burns will develop heterotopic ossification (HO), the pathologic formation of mature bone in soft tissues such as muscle, tendon, or even joint spaces. HO presents a significant barrier to quality of life, by delaying rehabilitation and causing chronic pain, open wounds, and joint immobility and contractures. Patients with traumatic burn injuries are at particular risk of developing upper extremity HO severely limiting their functional and vocational abilities. Patients who present with radiographic evidence of HO often undergo surgical excision, which yields dissatisfying results due to incomplete resection, a high risk of recurrence, and an inability to restore range of motion, or improve chronic pain. Drugs which exist can cause adverse healing effects in trauma patients, require long-term treatment, and are unable to be implemented in patients with the highest risk only. Thus, a need exists to prevent HO using therapeutics and minimize treatment duration to avoid adverse effects. The central goal of this grant is to inhibit the non-canonical (TAK1) and canonical (ALK2) bone morphogenetic (BMP) signaling pathways, two synergistic pathways critical for mesenchymal condensation and cartilage formation, using NG-25 and/or LDN-212854 respectively to prevent or eliminate HO and mitigate joint contractures. We will then demonstrate the ability of these therapeutics to be administered during specific phases of HO to simulate abbreviated, pulsed-dose treatment, or upon early diagnosis using near-infrared (NIR) imaging in our proven animal trauma models. Our overall goal is to generate a paradigm shift in our approach to patients at risk for HO, from delayed surgical excision or long-term treatment with non-specific inhibitors, to early preventative strategies which target high risk individuals with synergistic therapeutics. We hypothesize that early canonical and non-canonical BMP signaling are critical for HO formation and that inhibitors of both BMP pathways will prevent HO when administered early after injury.

2. **KEYWORDS:** Provide a brief list of keywords (limit to 20 words).

Heterotopic Ossification, Tak1, Alk2, BMP, near-infrared imaging

3. **ACCOMPLISHMENTS:** The PI is reminded that the recipient organization is required to obtain prior written approval from the awarding agency Grants Officer whenever there are significant changes in the project or its direction.

What were the major goals of the project?
List the major goals of the project as stated in the approved SOW. If the application listed milestones/target dates for important activities or phases of the project, identify these dates and show actual completion dates or the percentage of completion.

Major Task 1: Performing efficacy studies of NG-25 and LDN-212854 in rodent models of traumatic HO.

a. Perform longitudinal efficacy studies of NG-25 and/or LDN-212854 in the rodent Burn/tenotomy model, assessed by range-of-motion and live animal microCT measurements.

b. Perform longitudinal efficacy studies of NG-25 and/or LDN- 212854 in the rat blast/amputation model, assessed by histology and live animal microCT measurements.

Major Task 2: Performing *in vitro* treatment of mouse and rat HO and control MSCs with NG-25 and/or LDN-212854 for chondrogenic and osteogenic differentiation studies.

Major Task 3: Bioinformatics and biostatistics processing of heterotopic bone microCT radiographic density, osteogenic and chondrogenic gene and protein expression.

Major Task 4: Procurement of tissue from blast- and burn-mediated HO models without treatment at weekly time points.

Major Task 5: Histologic analysis of non-canonical and canonical BMP signaling in blast- and burn-mediated HO models without treatment at weekly time points.

Major Task 6: Pulsed-dose treatment of NG-25 and/or LDN-212854 in blast/amputation and EDHS206 and/or LDN-212854 in burn/tenotomy models with data analysis with biostatistical analysis.

Major Task 7: Near-infrared (NIR)-guided treatment of animal models with EDHS206 or NG025 and/or LDN-212854.

Major Task 8: Bioinformatics and biostatistics processing of heterotopic bone microCT radiographic density with NIR-guided treatment

What was accomplished under these goals?

Major Task 1: Performing efficacy studies of NG-25 and LDN-212854 in rodent models of traumatic HO.
Major Task 3: Bioinformatics and biostatistics processing of heterotopic bone microCT radiographic density, osteogenic and chondrogenic gene and protein expression.
Major Task 4: Procurement of tissue from blast- and burn-mediated HO models without treatment at weekly time points.

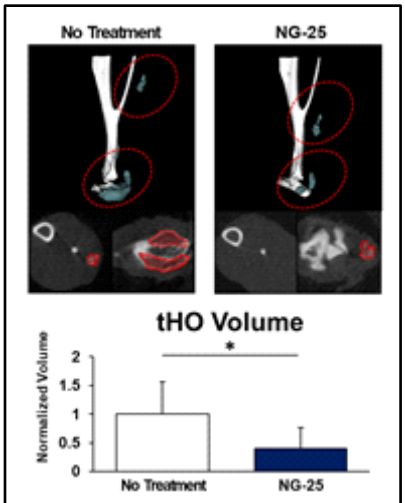

Fig. 1. MicroCT of HO site after burn/tenotomy with and without NG-25 treatment. Findings: NG-25 decreases total HO volume.

Objective: To prophylax against HO in an animal model of trauma-induced HO with burn/tenotomy injury using small-molecule inhibition of non-canonical (TAK1) or canonical (ALK2) bone morphogenetic protein (BMP) signaling separately or as combination therapy.
Methodology: All animal procedures were carried out in accordance with the guidelines provided in the Guide for the Use and Care of Laboratory Animals from the Institute for Laboratory Animal Research (ILAR, 2011) and were approved by the Institutional Animal Care and Use Committee of the University of Michigan (PRO0007930). All animals were housed in IACUC-supervised facilities, not to exceed five mice housed per cage at 72°F±4°F, receiving 12 hours of light exposure each day, with no diet restrictions. For all *in vitro*

and *in vivo* studies requiring wild type mice, young adult (6-8 weeks old) C57BL/6J mice were purchased from The Jackson Laboratory.
Partial-thickness scald burn injury was administered to animals according to a previously described protocol.(*16, 47*) Briefly, mice were anesthetized with inhaled isoflurane. Dorsal hair was closely clipped and an aluminum block heated to 60°C was exposed to the dorsal region over 30% of the total body surface area for 18 seconds to achieve a partial thickness burn injury. Each mouse then received a concurrent sterile dorsal hind limb tendon transection at the midpoint of the Achilles tendon (Achilles' tenotomy) with placement of a single 5-0 vicryl suture to close the skin. Pain management was achieved with subcutaneous injections of buprenorphine (Buprenex; Reckitt Benckiser Pharmaceuticals Inc.) every 8-12 hours for 48 hours post operatively.
Mice treated with NG-25, a TAK1 inhibitor demonstrated less end time point HO than control in our burn/tenotomy model (**Fig. 1**) and in our blast/amputation model (**Fig. 2**). This is an important validation that our therapeutic is working in the mechanism we hypothesized.

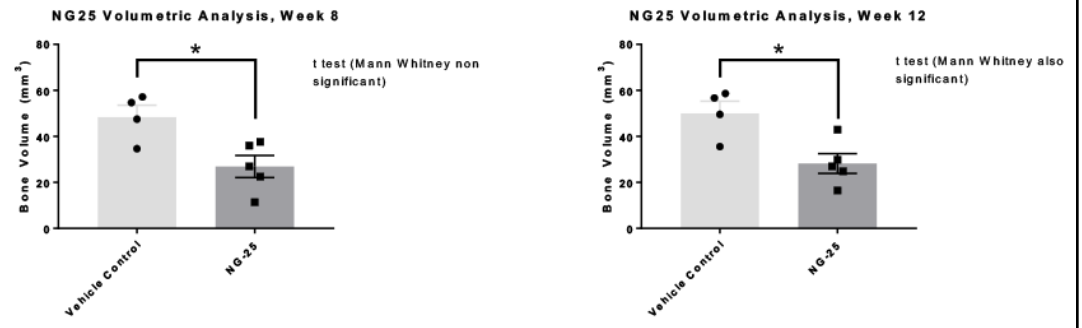

Fig. 2 MicroCT of rat blast/amputation followed by NG-25 treatment or vehicle control at 8 and 12 weeks.

Major Task 2: Performing *in vitro* treatment of mouse and rat HO and control MSCs with NG-25 and/or LDN-212854 for chondrogenic and osteogenic differentiation studies.
Objective:

Objective: To validate the effect of TAK1 inhibition of MSCs *in vitro*.

Methodology: All animal procedures were carried out in accordance with the guidelines provided in the Guide for the Use and Care of Laboratory Animals from the Institute for Laboratory Animal Research (ILAR, 2011) and were approved by the Institutional Animal Care and Use Committee of the Naval Medical Research Center (15-OUMD-19s). All animals were single housed in VSP-supervised facilities, not to exceed 72°F±4°F, receiving 12 hours of light exposure each day, with no diet restrictions. For adult (8-12 weeks old) rats were purchased from Taconic.Blast and amputation injury was administered to animals according to a previously described protocol (15-OUMD-19s). Briefly, rats were anesthetized with inhaled isoflurane and given Buprenex before receiving a 120±7 kPa blast. Rats were recovered and transferred to surgery room where they were anesthetized with isoflurane and received a fracture on the hind-

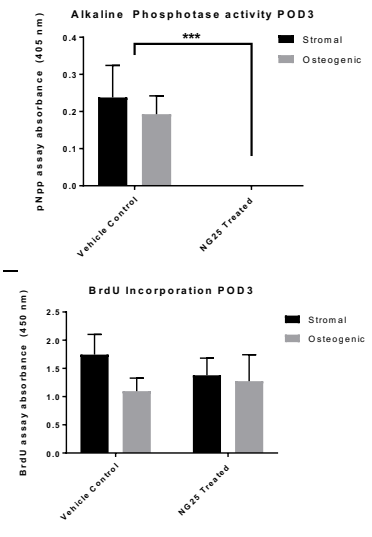

Fig. 3. NG-25 treatment resulted in the complete absence of alkaline phosphatase activity in a pNpp assay. This loss of activity was not due to a reduction in proliferation of the isolated MSCs as a BrdU incorporation assay showed no difference between NG-25 treated animals and controls.

limb femur followed by crush injury amputation through the zone of injury before being closed. Pain management was achieved with subcutaneous injections of buprenorphine SR every 48-72 hrs and then BID for 5-9 days or as needed.

Results:

MSCs from injured muscle (n=4 per time point) were successfully isolated and utilized in CTP, pNpp and BrdU incorporation assays. BrdU and pNpp assays have been completed. MSCs isolated from POD3 animals receiving NG-25 had a complete absence of alkaline phosphatase activity suggesting a failure to become osteogenic (**Fig. 3**). This was not due to a change in proliferation rate, as there was no difference in MSCs from POD3 animals' total BrdU incorporation (**Fig. 3**). There was also no difference in either assay between cells cultured in stromal (expansion) media and osteogenic (differentiation) media (**Fig. 3**).

Muscle taken for gene analysis has been processed for RNA isolation, confirmed isolated RNA was of high quality, cDNA synthesis from isolated RNA, and completed qPCR (n=4 per time point). Preliminary data analysis of qPCR data has been completed. 5 genes were significantly changed in the NG25 treated animals compared to the vehicle controls at POD3, 1 gene at POD7, and 36 genes at POD10 (**Fig. 4**). We saw no significant changes in any of the HO implicated proteins examined. However, there were trends towards a reduction in Runx2 and IBSP expression at early time points and a trending increase in PDGF-AA expression at early time points.

Kinetic assay vehicle controls were completed in the NG-25 treatment rat blast-amputation heterotopic ossification model. The assayed time points were 3, 7, and 10 days post injury. Tissue isolation included blood for CBC, blood chemistry, and Luminex, isolation of injured muscle surrounding the amputation site and contralateral muscle for gene

POD 3

Gene Name	p value	Treatment Group	Mean
Phex	0.009239119	Control	0.528778
		Treated	1.578747
Ccl3	0.042913992	Control	101.7838
		Treated	5.166702
Ibsp	0.043109692	Control	1.059582
		Treated	9.165922
Comp	0.043278397	Control	4.509548
		Treated	14.43521
Bmp4	0.048893600	Control	0.354851
		Treated	0.886076

POD 7

Gene Name	p value	Treatment Group	Mean
Ibsp	0.024197622	Control	8.7121642
		Treated	1.4832684

POD 10

Gene Name	p value	Treatment Group	Mean
Jag1	0.0000514	Control	0.0135512
		Treated	2.2816881
Il6	0.0003924	Control	222.95255
		Treated	1.8960118
Ptk2	0.0009861	Control	0.0358257
		Treated	0.9103122
Vegfa	0.0011620	Control	0.0021252
		Treated	0.5368869
Smurf2	0.0016337	Control	0.0115591
		Treated	1.4366721
Hdac1	0.0016760	Control	0.0173558
		Treated	3.7223458
Angpt2	0.0016818	Control	0.0649085
		Treated	1.4521801
Ibsp	0.0018528	Control	196.72365
		Treated	0.7022873
Lrp5	0.0019080	Control	0.0109147
		Treated	0.587754
Il10	0.0020458	Control	53.984263
		Treated	2.4800595
Fabp4	0.0024332	Control	0.0026601
		Treated	0.4533657
Col1a1	0.0033262	Control	0.0049019
		Treated	1.5265262
Tgfb1	0.0044436	Control	0.0645618
		Treated	2.136961
Lep	0.0052411	Control	13.884189
		Treated	0.229249
Tert	0.0052511	Control	49.482685
		Treated	1.3006969
Bglap	0.0059866	Control	494.33888
		Treated	3.5114619
Flt1	0.0061611	Control	0.0078094
		Treated	0.9343641
Tac1	0.0074732	Control	9297.3222
		Treated	2.1711634
Gusb	0.0111152	Control	0.015545
		Treated	4.4046506
Il1b	0.0111323	Control	0.2718997
		Treated	11.093751
Col2a1	0.0119465	Control	1.9593849
		Treated	0.0761021
Sox2	0.0120410	Control	430.54992
		Treated	2.1220642
Cd44	0.0136255	Control	0.1067226
		Treated	2.605886
Col10a1	0.0166422	Control	718.57479
		Treated	0.8236405
Sparc	0.0171530	Control	0.0182997
		Treated	2.6394705
Bmp4	0.0181239	Control	0.0101525
		Treated	1.4547738
Itgam	0.0189335	Control	0.0634917
		Treated	6.2317587
PPC	0.0210160	Control	3.9519445
		Treated	1.2952009
Cebpa	0.0212102	Control	53.288915
		Treated	2.7444104
Bmp2	0.0213969	Control	10.826567
		Treated	0.6459167
Smad3	0.0269178	Control	1581.0941
		Treated	6.845238
Omd	0.0293826	Control	0.0572273
		Treated	0.8935482
Pdgfa	0.0390047	Control	0.0277848
		Treated	1.218545
Itga2	0.0398598	Control	0.1713607
		Treated	1.6492852
Adipor1	0.0466021	Control	0.0415046
		Treated	0.4624931
Ptch1	0.0479071	Control	0.1195962
		Treated	1.1087927

Fig. 4. Significantly changed genes in the NG-25 treated animals when compared to the vehicle control at POD3, POD7 and POD10.

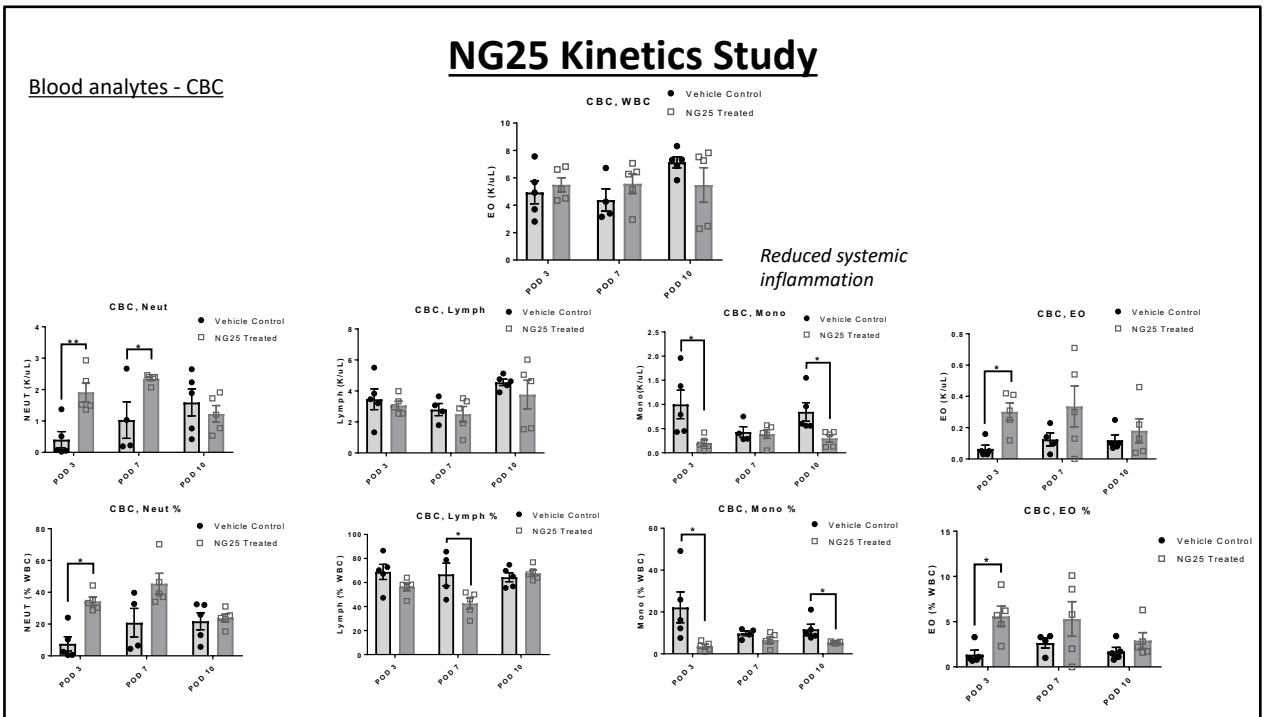

Fig. 5. Blood analyte kinetic study.

and protein analysis, injured muscle for MSC isolation, and whole limb isolation for histology. Blood and serum was isolated from the animals and run for total blood counts, blood chemistries and a 23 analyte Luminex panel. CBC analysis revealed an increase in neutrophil numbers at POD3 and POD7 and a decrease in monocytes at POD3 and POD10 (**Fig. 5**). Blood chemistries revealed a drop in total protein at POD10 and a reduction in albumin at POD7 .

We next performed protein arrays of the same analyses as our gene analyses. We did not find any differences in the protein levels between groups (**Fig. 6**). Importantly we did see a significant difference in CFUs in MSCs treated with NG-25 compared to vehicle control (**Fig. 7**).

Next, MSCs were harvested from the soft tissue of the injured extremity. All tissue was mechanically minced, digested with collagenase A and dispase, and subsequently plated. Cells used were all passage 2 through 6. Cells were grown in Chondrogenic differentiation medium with or without TGFB1. Micromass pellets were harvested, sectioned and stained with Alcian blue.

In vitro, Chondrogenic differentiation medium with TGFB1 and without TGFB1 lead to successful Chondrogenic differentiation. We found that genetic *Tak1* knockout decreased chondrogenic differentiation by micromass as well as decreased chondrogenic signaling (**Fig. 8**). Importantly, therapeutic TAK1 inhibition with NG-25 significantly decreased chondrogenic differentiation as well as chondrogenic gene expression (**Fig. 9**).

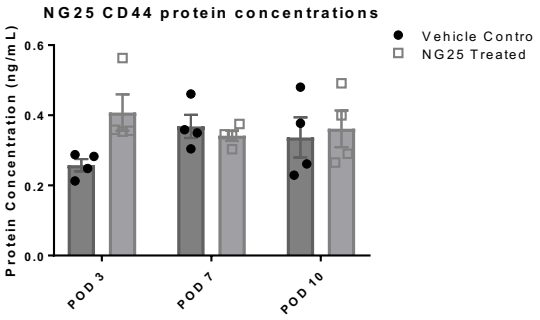

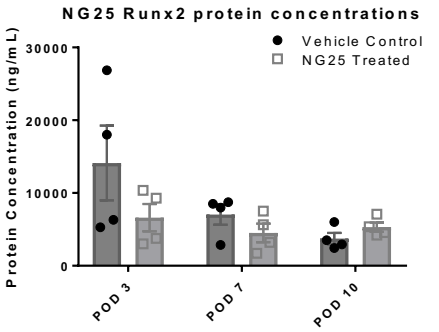

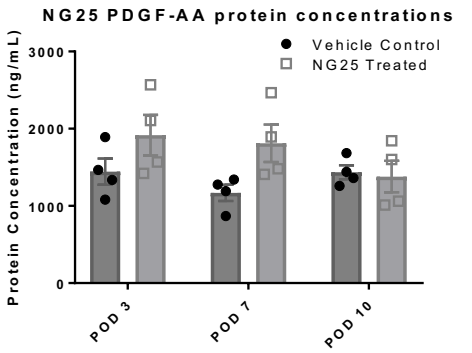

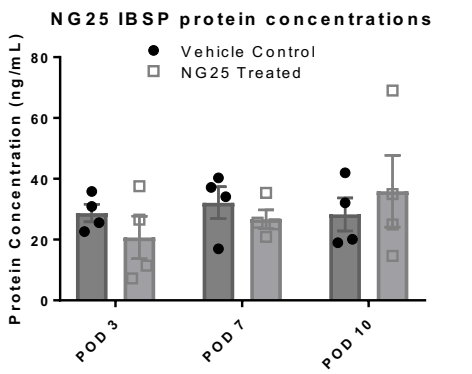

Fig. 6 Protein expression data from vehicle control and NG-25 treated animals. Proteins examined include PDGF-AA (A), CD44 (B), Runx2 (C) and IBSP (D).

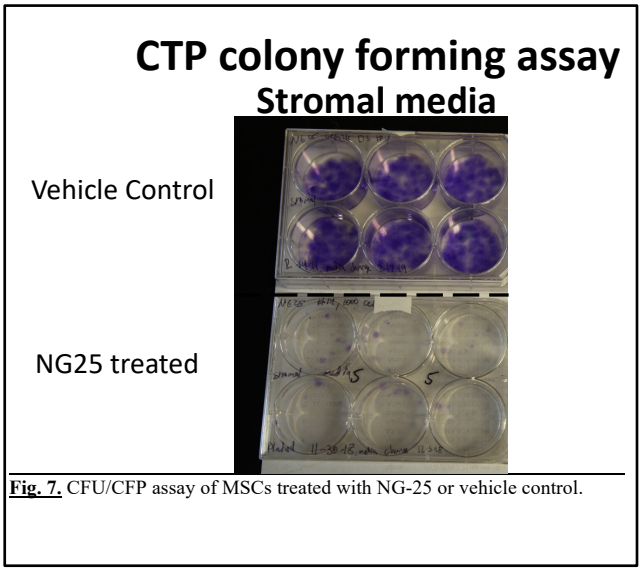

Fig. 7. CFU/CFP assay of MSCs treated with NG-25 or vehicle control.

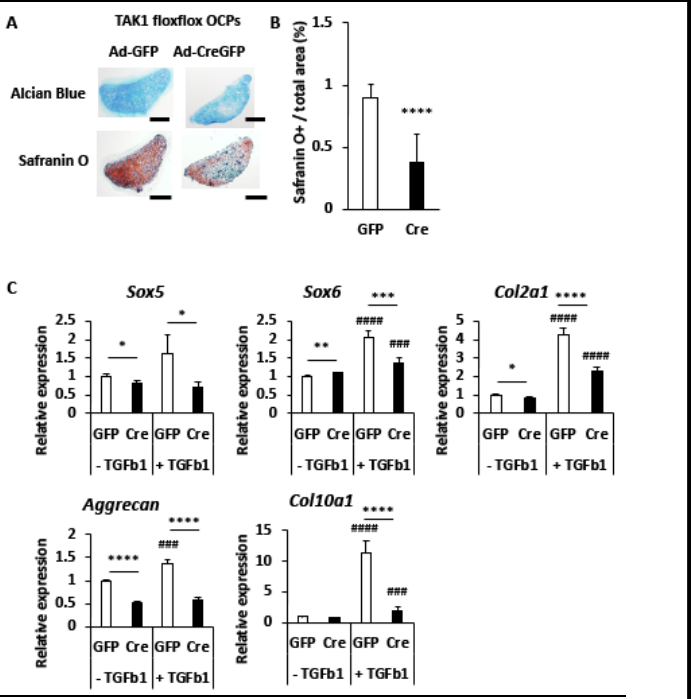

Fig. 8 Tak1 deletion decreases chondrogenic differentiation and signaling. **A.** Micromass assay of pre-osteoblasts from mice with Tak1 deletion compared to AdGFP controls. **B.** Quantification of cartilage in micromass in cells with Tak1 deletion or littermate controls. **C.** Chondrogenic gene expression by qRT PCR from micromass pellets of cells with *Tak1* deletion or lit AdGFP controls.

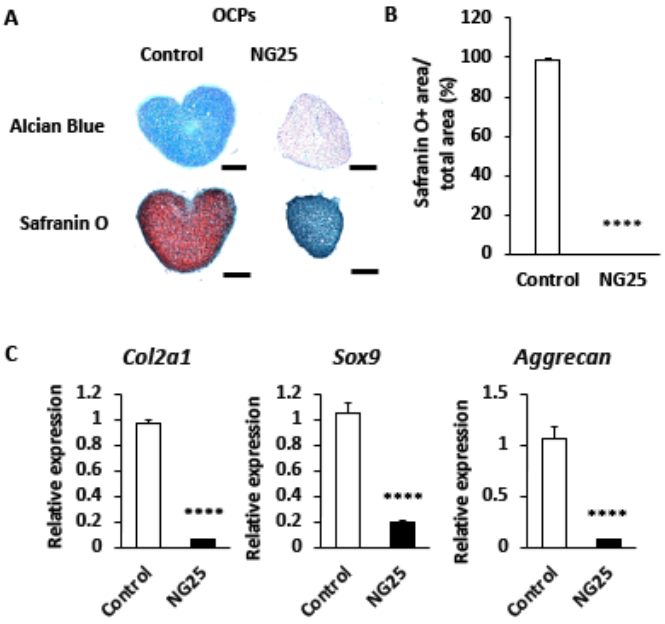

Fig. 9 Tak1 inhibition with NG-25 decreases chondrogenic differentiation and signaling. A. Micromass assay of pre-osteoblasts from mice treated with NG-25 or vehicle control. **B.** Quantification of cartilage in micromass in cells with Tak1 deletion or littermate controls. **C.** Chondrogenic gene expression by qRT PCR from micromass pellets of cells with *Tak1* deletion or lit AdGFP controls.

Major Task 5: Histologic analysis of non-canonical and canonical BMP signaling in blast- and burn-mediated HO models.

Partial-thickness scald burn injury was administered to animals according to a previously described protocol.(*16, 47*) Briefly, mice were anesthetized with inhaled isoflurane. Dorsal hair was closely clipped and an aluminum block heated to 60°C was exposed to the dorsal region over 30% of the total body surface area for 18 seconds to achieve a partial thickness burn injury. Each mouse then received a concurrent sterile dorsal hind limb tendon transection at the midpoint of the Achilles tendon (Achilles' tenotomy) with placement of a single 5-0 vicryl suture to close the skin. Mice were treated with NG-25 or vehicle control. We saw significantly less pre-HO cartilage in the NG-25 treated mice (**Fig. 10**). This was consistent with a decrease in pre-HO cartilage in the our blast/amputation model (**Fig. 11**).

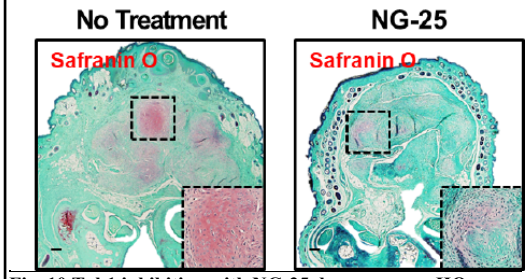

Fig. 10 Tak1 inhibition with NG-25 decreases pre-HO chondrogenic differentiation and signaling. Histologic analysis of HO site 3 weeks after burn/tenotomy with and without NG-25 treatment. **Findings: NG-25 decrease pre-HO cartilage formation.**

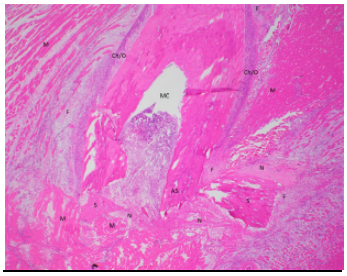

Fig. 11 Tak1 inhibition with NG-25 mitigates pre-HO cartilage formation in blast/amputation model. Histologic analysis of HO 1 week after blast/amputation with NG-25 treatment. **Findings: NG-25 decreases pre-HO cartilage formation.**

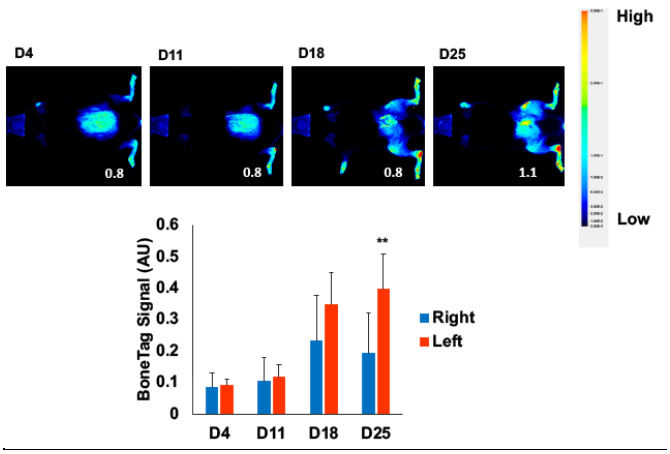

Fig. 12. NIR of HO site after burn/tenotomy. Findings: NIR can detect early changes associated with HO at 2 weeks after injury which is several weeks prior to detection with microCT .

Major Task 7: Near-infrared (NIR)-guided treatment of animal models with NG-25.

In order to determine the optimal timing to initiate treatment, we performed NIR imaging. Comparing the HO site compared to the uninjured non-HO hindlimb. We found that starting at day18, we began to notice an increase in pre-HO changes with statistical significance achieved at day 25 (**Fig. 12**).

Major Task 6 and 8: Pulsed-dose treatment of NG-25 in blast/amputation and burn/tenotomy models with data analysis with biostatistical analysis.

Bioinformatics and biostatistics processing of heterotopic bone microCT radiographic density with NIR-guided treatment

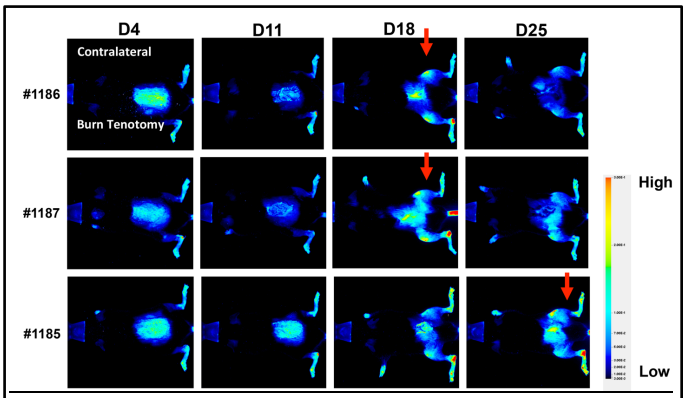

Fig. 13. NIR of HO site after burn/tenotomy. Findings: NIR can detect early changes associated with HO at 2 weeks after injury which is several weeks prior to detection with microCT .

Partial-thickness scald burn injury was administered to animals according to a previously described protocol.(*16, 47*) Briefly, mice were anesthetized with inhaled isoflurane. Dorsal hair was closely clipped and an aluminum block heated to 60°C was exposed to the dorsal region over 30% of the total body surface area for 18 seconds to achieve a partial thickness burn injury. Each mouse then received a concurrent sterile dorsal hind limb tendon transection at the midpoint of the Achilles tendon (Achilles' tenotomy) with placement of a single 5-0 vicryl suture to close the skin. Pain management was achieved with subcutaneous injections of buprenorphine (Buprenex; Reckitt Benckiser Pharmaceuticals Inc.) every 8-12 hours for 48 hours post operatively. NIR imaging was performed using Osteosense injection followed by imaging on the Pearl NIR scanner. This was performed on a weekly basis. We found that the injured had 4x the level of signal compared to the uninjured control side at day 18 in 2 of the mice and at day 25 in 1 of the mice (**Fig. 13**).

Next, we did pulse treatment of NG-25 to see if we could use shorter treatment regimens. We found that pulse treatments was not as effective as continuous treatments (**Fig. 14**).

What opportunities for training and professional development has the project provided?

This has allowed for several laboratory members to attend the annual MHSRS meeting. Additionally, this led to Dr. Levi being awarded the ASBMR Fuller Albright Young Investigator

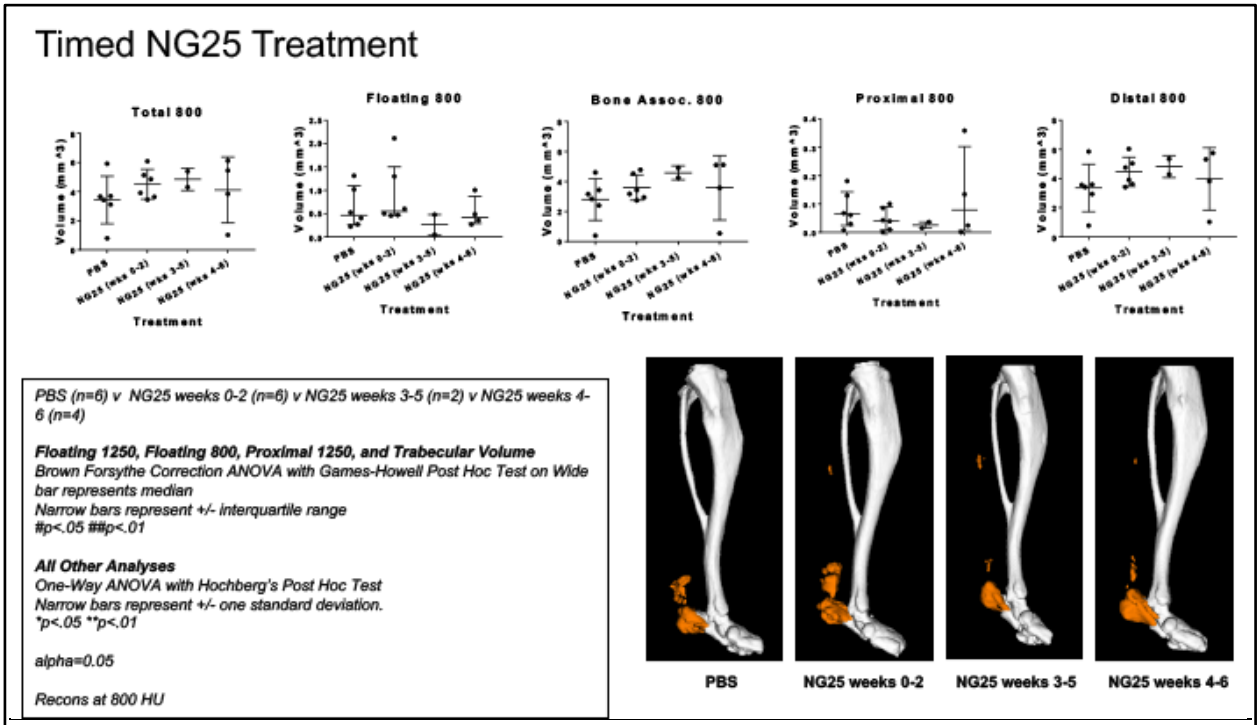

Fig. 14. **MicroCT of burn/tenotomy followed by timed treatments.**

Award for being one of the most promising bone biologists. This enabled him to attend the annual ASBMR meeting. Additionally, Dr. Levi has attended the University of Michigan Leadership Development Program through the Department of Surgery.

How were the results disseminated to communities of interest?
If there is nothing significant to report during this reporting period, state "Nothing to Report."

Describe how the results were disseminated to communities of interest. Include any outreach activities that were undertaken to reach members of communities who are not usually aware of these project activities, for the purpose of enhancing public understanding and increasing interest in learning and careers in science, technology, and the humanities.

Results were disseminated through annual meetings including MHSRS, ASBMR, Gordon Conference Bone and Teeth, Plastic Surgery Research Council and Orthopedic Research Society.

What do you plan to do during the next reporting period to accomplish the goals?
If this is the final report, state "Nothing to Report."

Nothing to report

4. **IMPACT:** Describe distinctive contributions, major accomplishments, innovations, successes, or any change in practice or behavior that has come about as a result of the project relative to:

What was the impact on the development of the principal discipline(s) of the project?
If there is nothing significant to report during this reporting period, state "Nothing to Report."

We have now definitely shown that targeting TAK1 significantly decreases HO progenitor cell chondrogenic and osteogenic differentiation in vitro across multiple cell lines. More importantly, we have shown that TAK1 inhibition with pre-clinical NG-25 significantly decreases HO formation. As new Tak1 inhibitors continue in development and through the FDA process, we believe they can be used to prophylax against HO in high risk patients.

What was the impact on other disciplines?
If there is nothing significant to report during this reporting period, state "Nothing to Report."

Describe how the findings, results, or techniques that were developed or improved, or other products from the project made an impact or are likely to make an impact on other disciplines.

Nothing to report

What was the impact on technology transfer?
If there is nothing significant to report during this reporting period, state "Nothing to Report."

Nothing to report

What was the impact on society beyond science and technology?
If there is nothing significant to report during this reporting period, state "Nothing to Report."

Nothing to report

5. **CHANGES/PROBLEMS:** The Project Director/Principal Investigator (PD/PI) is reminded that the recipient organization is required to obtain prior written approval from the awarding agency Grants Officer whenever there are significant changes in the project or its direction. If not previously reported in writing, provide the following additional information or state, "Nothing to Report," if applicable:

Changes in approach and reasons for change
Describe any changes in approach during the reporting period and reasons for these changes. Remember that significant changes in objectives and scope require prior approval of the agency.

Nothing to report

Actual or anticipated problems or delays and actions or plans to resolve them
Describe problems or delays encountered during the reporting period and actions or plans to resolve them.

Nothing to report

Changes that had a significant impact on expenditures

Nothing to report

Significant changes in use or care of human subjects, vertebrate animals, biohazards, and/or select agents

Significant changes in use or care of human subjects

Nothing to report

Significant changes in use or care of vertebrate animals.

Nothing to report

Significant changes in use of biohazards and/or select agents

Nothing to report

6. **PRODUCTS:** List any products resulting from the project during the reporting period. If there is nothing to report under a particular item, state "Nothing to Report."

- **Publications, conference papers, and presentations**

Sung Hsieh HH, Agarwal S, Cholok DJ, Loder SJ, Kaneko K, Huber A, Chung MT, Ranganathan K, Habbouche J, Li J, Butts J, Reimer J, Kaura A, Drake J, Breuler C, Priest CR, Nguyen J, Brownley C, Peterson J, Ozgurel SU, Niknafs YS, Li S, Inagaki M, Scott G, Krebsbach P, Longaker MT, Westover K, Gray N, Ninomiya-Tsuji J, Mishina Y, **Levi B**. Coordinating Tissue Regeneration through TGF-β Activated Kinase 1 (TAK1) Inactivation and Re-activation. *Stem Cells.* 2019 Jun;37(6):766-778. PMID: 30786091.

Books or other non-periodical, one-time publications.

1. Loder S, Agarwal S, Hsieh H, Cholok D, Chung M, Li J, Breuler C, Priest C, Ranganathan K, Habbouche J, Kaura A, Butts J, Li S, Mishina Y, **Levi B**. Loss Of TGF-beta Activated Kinase (TAK1) Activity Induces Cellular Proliferation And Diminishes Differentiation During Bone Healing. *Plast Reconstr Surg Glob Open*. 2017 May 1;5(4 Suppl):90-91. PMCID: PMC5417975.
2. Hsung HH, Agarwal S, Loder S, Drak J, Cholok D, Li J, Ranganathan K, Li S , Mishina Y, **Levi B**. **Noncanonical BMP Signaling Regulates Endochondral Bone Development and Trauma-Induced Heterotopic Ossification**. *Plast Reconstr Surg Glob Open*. 2017 Mar 8;5(2 Suppl):45. PMCID: PMC5361372.

Other publications, conference papers, and presentations.

1. Agarwal S, Loder S, Cholok D, Breuler C, Chung M, Brownley C, Peterson J, Li J, Hsu Ranganathan K, Priest C, Li S, Mishina Y, **Levi B**. *A Translational Strategy Targeting I BMP Receptors to Prevent Heterotopic Ossification.* PSRC Annual Meeting 2017, Durham, North Carolina.
2. Loder S, Agarwal S, Hsung H, Cholok D, Chung M, Li J, Breuler C, Priest C, Ranganathan K, Habbouche J, Kaura A, Butts J, Li S, Mishina Y, **Levi B**. *Loss of TGF- beta Activated Kinase (TAK1) Activity Induces Cellular Proliferation and Diminishes Differentiation During Bone Healing.* PSRC Annual Meeting, Durham, NC. May 2017.
3. Mishina Y, Hsieh H, Agarwal S, Pan H, and **Levi B**. *Coordinating Tissue Regeneration Through TGF-beta Activated Kinase 1 (TAK1) Inactivation and Reactivation*. Gordon Research Conference, Galveston, TX. February 2018.
4. Mishina Y and Levi B. Role of TAK1 in FOP. iFOPA meeting, Orlando, FL. November 2019.

- **Website(s) or other Internet site(s)**

www.burnwoundlab.com

- **Technologies or techniques**
  Identify technologies or techniques that resulted from the research activities. In addition to a description of the technologies or techniques, describe how they will be shared.

None

- **Inventions, patent applications, and/or licenses**

None

- **Other Products**

None

7. PARTICIPANTS & OTHER COLLABORATING ORGANIZATIONS

What individuals have worked on the project?

Benjamin Levi, MD
Matthew Bradley, MD
Ryan Haskins, PhD
John Mares
Shuli Li, PhD
Keegan Loveless
Babita Prajuli
Peter Luang
Nicole Edwards, PhD
Philip Spreadborough, MD

Has there been a change in the active other support of the PD/PI(s) or senior/key personnel since the last reporting period?

Nothing to report

What other organizations were involved as partners?

Nothing to report

8. SPECIAL REPORTING REQUIREMENTS

9. APPENDICES

Appendix A: quad chart

STEM CELLS®

REGENERATIVE MEDICINE

Coordinating Tissue Regeneration Through Transforming Growth Factor-β Activated Kinase 1 Inactivation and Reactivation

HSIAO HSIN SUNG HSIEH,[a,b,i,*] SHAILESH AGARWAL,[a,*] DAVID J. CHOLOK,[a] SHAWN J. LODER,[a] KIEKO KANEKO,[a] AMANDA HUBER,[a] MICHAEL T. CHUNG,[a] KAVITHA RANGANATHAN,[a] JOE HABBOUCHE,[a] JOHN LI,[a] JONATHAN BUTTS,[a] JONATHAN REIMER,[a] ARMINDER KAURA,[a] JAMES DRAKE,[a] CHRISTOPHER BREULER,[a] CAITLIN R. PRIEST,[a] JOE NGUYEN,[b] CAMERON BROWNLEY,[a] JONATHAN PETERSON,[a] SERRA UCER OZGUREL,[a] YASHAR S. NIKNAFS,[a] SHULI LI,[a] MAIKO INAGAKI,[c] GREG SCOTT,[d] PAUL H. KREBSBACH,[f] MICHAEL T. LONGAKER,[g] KENNETH WESTOVER,[h] NATHANAEL GRAY,[e] JUN NINOMIYA-TSUJI,[c] YUJI MISHINA,[b] BENJAMIN LEVI[a]

[a]Department of Surgery, University of Michigan, Ann Arbor, Michigan, USA; [b]School of Dentistry, University of Michigan, Ann Arbor, Michigan, USA; [c]Department of Environmental and Molecular Toxicology, North Carolina State University, Raleigh, North Carolina, USA; [d]Knock Out Core, National Institute of Environmental Health Sciences, National Institutes of Health, Research Triangle Park, North Carolina, USA; [e]Dana-Farber Cancer Institute, Boston, Massachusetts, USA; [f]Section of Periodontics, UCLA School of Dentistry, Los Angeles, California, USA; [g]Institute for Stem Cell Biology and Regenerative Medicine, Stanford University School of Medicine, Stanford, California, USA; [h]Department of Biochemistry, University of Texas Southwestern, Dallas, Texas, USA; [i]Experimental Rheumatology Department, Radboud University Medical Center, Nijmegen, The Netherlands

[*]Co-first authors.

Correspondence: Benjamin Levi, M.D., Department of Surgery, University of Michigan, 1150 W Medical Center Dr. MSRB 2 A 574, Ann Arbor, Michigan 48109, USA. Telephone: 734-936-5890; e-mail: blevi@med.umich.edu; or Yuji Mishina, Ph.D., School of Dentistry, University of Michigan, 1011 N. University Ave. Dent 4222A, Ann Arbor, Michigan 48109, USA. Telephone: 734-763-5579; e-mail: mishina@umich.edu

Received February 18, 2018; accepted for publication November 24, 2018; first published online February 20, 2019.

http://dx.doi.org/10.1002/stem.2991

Key Words. Cellular proliferation • Differentiation • Progenitor cells • Proliferation • Stem/progenitor cell • Tissue regeneration

ABSTRACT

Aberrant wound healing presents as inappropriate or insufficient tissue formation. Using a model of musculoskeletal injury, we demonstrate that loss of transforming growth factor-β activated kinase 1 (TAK1) signaling reduces inappropriate tissue formation (heterotopic ossification) through reduced cellular differentiation. Upon identifying increased proliferation with loss of TAK1 signaling, we considered a regenerative approach to address insufficient tissue production through coordinated inactivation of TAK1 to promote cellular proliferation, followed by reactivation to elicit differentiation and extracellular matrix production. Although the current regenerative medicine paradigm is centered on the effects of drug treatment ("drug on"), the impact of drug withdrawal ("drug off") implicit in these regimens is unknown. Because current TAK1 inhibitors are unable to phenocopy genetic Tak1 loss, we introduce the dual-inducible COmbinational Sequential Inversion ENgineering (COSIEN) mouse model. The COSIEN mouse model, which allows us to study the response to targeted drug treatment ("drug on") and subsequent withdrawal ("drug off") through genetic modification, was used here to inactivate and reactivate Tak1 with the purpose of augmenting tissue regeneration in a calvarial defect model. Our study reveals the importance of both the "drug on" (Cre-mediated inactivation) and "drug off" (Flp-mediated reactivation) states during regenerative therapy using a mouse model with broad utility to study targeted therapies for disease. STEM CELLS *2019;37:766–778*

SIGNIFICANCE STATEMENT

This study targets the transforming growth factor-β activated kinase 1 (TAK1) pathway to reduce heterotopic ossification, a pathologic condition in which bone develops within muscle or soft tissues. It shows that *Tak1* knockout leads to cellular proliferation; this can be harnessed to increase the number of cells present at the injury site. Using a mouse model, the *Tak1* gene was inactivated and reactivated. It showed that inactivation and reactivation of *Tak1* can improve bony healing through the coordination of increased proliferation (inactivation) followed by differentiation (reactivation). This approach elucidates a new paradigm in regenerative medicine in which coordination between treatment and withdrawal of treatment can augment healing.

INTRODUCTION

Normal tissue regeneration requires coordination between cellular proliferation and subsequent differentiation. Any disturbance of this coordinated balance leads to pathologic wound healing after injury, as observed in patients with heterotopic ossification (HO). Current state of knowledge on tissue engineering-based approaches for wound regeneration is based on cell transplantation and biomaterials [1–3]. Additionally, approaches with small-molecules modify pathways responsible for cellular proliferation/apoptosis [4–7] or differentiation [8–13], but typically not both.

HO is a condition in which extraskeletal bone forms in response to local tissue injury; although HO has primarily been studied in the

context of genetic mutations in type I bone morphogenetic protein receptors [14–17], it also is known to form in patients after severe trauma without genetic mutations (e.g., trauma-induced HO [tHO]) [14, 18–20]. Recently, we have shown that tHO is caused by pathologic cellular proliferation and subsequent differentiation through a cartilaginous intermediary [14, 20], prompting us to study transforming growth factor-β (TGF-β), a known mediator of cartilage formation [21–27], in HO. Here, we specifically focus on the TGF-β activated kinase 1 (TAK1) signaling pathway [23, 24, 26, 28] to coordinate cellular proliferation and differentiation to reduce HO or improve bony calvarial healing.

TGF-β activating kinase 1 (TAK1) is a key regulator of mitogen-activated protein kinases (MAPK) kinase activation in TGF-β and bone morphogenetic protein (BMP) signaling pathways [27]. In adults, TAK1 has diverse roles spanning inflammation and the immune response, wound healing, fibrosis, and oncogenesis [23, 24, 26, 28–31]. During development, TAK1 is critical for the proliferation and maturation of bone, cartilage, skin, and vascular endothelium and is a major regulator of the condensation, proliferation, and differentiation of early mesenchymal population. Mechanistically, TAK1 transduces signals to several downstream signaling cascades, including mitogen-activated protein kinase 4/7 (MKK4/7)-c-Jun N-terminal kinases, MKK3/6-p38 MAPK, and nuclear factor-kappa β (NF-κB)-inducing kinase-IκB kinase. TAK1 is necessary for propagation of both SMAD-dependent and independent (p38 MAPK) BMP signaling pathways [23, 24, 26, 28]. Furthermore, TAK1 is central to cytokine-induced activation of NF-κB via interleukin 1-β [32].

To coordinate the TAK1 signaling pathway, we generated a novel genetic mouse model (Cre/Flp mouse) which allows Tak1 to be knocked out using Cre/lox technology (fx) and subsequently reactivated using Flp/Frt technology (frt) [32]. The resulted COmbinational Sequential Inversion ENgineering (COSIEN) mouse allows us to elucidate a "drug on"/"drug off" therapeutic paradigm to optimize bone regeneration. Our findings suggest that precise regulation of TAK1 allows for control of the proliferation-differentiation switch in stem cell/progenitor population at the wound site (Supporting Information Fig. S1). Our system demonstrates the potential for therapeutic leverage of a central regulatory protein to affect wound healing in both physiologic and pathologic models.

Materials and Methods

Ethics Statement

All animal experiments described were approved by the University Committee on Use and Care of Animals at the University of Michigan-Ann Arbor (Protocols: #05909, 05182, 05716, and 07715). This study was carried out in strict accordance with the recommendations in the Guide for the Use and Care of Laboratory Animals from the Institute for Laboratory Animal Research (2011). All animals were housed in Institutional Animal Care and Use Committees (IACUC)-supervised facilities, not to exceed five mice housed per cage at 18°C–22°C, 12-hour light–dark cycle with ad libitum access to food and water.

Animals

All mice used in this study were derived from a C57BL/6 background. Adult 6- to 8-week-old wild-type C57BL/6 (Charles River Laboratory, Boston, MA) mice were included as controls. Mutant mice used in this study included tamoxifen-inducible postnatal *Tak1* knockout (*Tak1* tmKO: *Ub.CreERT/Tak1*$^{fl\text{-}frt/fl\text{-}frt}$), conditional *Tak1* knockout (*Tak1* cKO: *Prx.Cre/Tak1*$^{fl\text{-}frt/fl\text{-}frt}$), dual inducible *Tak1* knockout (*Tak1*$^{fl\text{-}frt/fl\text{-}frt}$), and their respective littermate controls. All breeding was performed at the University of Michigan in facilities managed by the Unit for Laboratory Animal Medicine. Tail genomic DNA was used for genotyping.

Generation of Dual Inducible COSIEN Mouse for Inactivation and Reactivation of Tak1

Exon 2 of Tak1 was targeted because removal of exon 2 has been shown to be sufficient to disrupt gene function [30]. A 4.5-kb fragment containing intron 1 of Tak1 locus was polymerse chain reaction (PCR) amplified from 129SvEv genomic DNA with Phusion polymerase (New England Biolabs, Inc., MA). A 2.8-kb fragment containing exon 2 and 3.6-kb fragment containing intron 2 were PCR amplified. After amplification, these fragments were ligated with mutant loxP sites, mutant FRT sites, a PGK-Neo cassette, and DTA cassette to generate a targeting vector (Supporting Information Figs. S1, S2). The positions of the probes used for Southern analysis and positions of PCR genotyping primers are shown. The sizes of the restriction fragments detected by these probes in WT and targeted DNA are shown above or below the locus. A 5′ and 3′ loxP–FRT sites are marked with an *Eco*RV and a *Hind*III sites, respectively.

Since both loxP sites and FRT sites are placed in the locus in an opposite direction, recombinase-mediated DNA recombination flips the sequence between instead of its deletion. To avoid continuous flipping and allow for one-time recombination, we introduced mutations in each recognition site. Lox66 has mutations in five bases at the most 3′ region whereas Lox72 has mutations in the most 5′ region [38]. FRT GS1-1 has a single base change in 5′ arm whereas FRT GS2-1 has a single base change in 3′ arm [39]. Cre-mediated DNA recombination flips the sequence between Lox66 and Lox72, but after recombination, one of the resulted LoxP sequences bears mutations in both 5′ and 3′ arms, which no longer can be a substrate for Cre recombinase. Thus, exon 2 will be flipped by Cre recombinase only one time and gene function will be lost (Supporting Information Fig. S2). Flippase-mediated DNA recombination flips the sequence between FRT GS1-1 and FRT GS1-2. After recombination, one of the resulted FRT sequences bears mutations in both 5′ and 3′ arms to stop further recombination. Thus, exon 2 will be flipped back and gene function will be restored (Supporting Information Fig. S2). We named this system as COSIEN.

Linearized targeting vector was electroporated into 1.6×10^7 clones A3 of UG347 ES cells, which we established from 129SvEv blastocysts. Three hundred G418-resistant ES cell clones were initially screened by Southern blot and targeted ES cell clones were identified (Supporting Information Fig. S10A). The targeted ES clones were injected into blastocysts from C57BL/6 albino mice. The resulting chimeras were bred to C57BL/6 females and F1 agouti offspring were genotyped by Southern analyses. Three targeted clones were used for injection and one of them underwent germline transmission. Subsequently, mice heterozygous for *Tak1* floxed-FRTed allele (*Tak1*$^{fl\text{-}frt/wt}$; Supporting Information Fig. S10B) were intercrossed to obtain homozygous mice for *Tak1* floxed-FRTed allele (*Tak1*$^{fl\text{-}frt/fl\text{-}frt}$). The homozygous mice were obtained as an expected ratio

(25%, $n > 100$), suggesting that presence of the loxP, FRT, and the neo cassette does not influence gene activity.

When bred with a germline deleter Cre strain Meox2-Cre, all mice positive for the Cre showed a flipped band by genomic PCR (Supporting Information Fig. S10C). After segregation of Cre from the flipped *Tak1* allele (designated as $Tak1^{fc}$ allele, $Tak1^{fc/+}$ mice were bred with Meox2-Cre mice again. None of the $Tak1^{fc/+}$ mice carrying Cre showed the floxed band (200 bp) with *Tak1* G1/G2 primers indicating that the Cre-mediate DNA inversion occurs only one time ($n > 20$, data not shown). Homozygous mice for Tak1 Cre-flipped allele ($Tak1^{fc/fc}$) were generated by intercross of $Tak1^{fc/+}$ mice and resulted homozygous mice showed embryonic lethality around E9.5 similar to the *Tak1* homozygous null embryos reported earlier (data not shown). These suggesting that the *Tak1* floxed-FRTed allele can flip one time with Cre recombinase to disrupt gene function.

When bred with Flipper mice (carrying FLPe gene) [32], mice carrying both the $Tak1^{fx\text{-}frt}$ alleles and Flpe showed a flipped band by genomic PCR using TAK1 F6/G2 primers (Supporting Information Fig. S10D). Unlike the case of Meox2-Cre, we found some of them showed both floxed and flipped bands suggesting that DNA inversion mediated by FLPe may be less efficient than that by Cre (Supporting Information Fig. S10D, sample #4).

Injury Models

All mice received presurgical analgesia consisting of 0.1 mg/kg buprenorphine, followed by anesthesia with inhaled isoflurane, and close postoperative monitoring with analgesic administration. Experimental trauma model 1: burn/tenotomy (B/T) mice received a 30% total body surface area (TBSA) partial-thickness burn on the shaved dorsum followed by left hind limb Achilles' tendon transection [16]. The dorsum was burned using a metal block heated to 60°C and applied to the dorsum for 18 seconds continuously. The tenotomy site was closed with a single 5-0 vicryl suture placed through the skin only. *Ub.Cre/* $Tak1^{fl\text{-}frt/fl\text{-}frt}$ and littermate control mice received 175 mg/kg tamoxifen 7 and 3 days prior the surgery and 7, 14, and 21 days after the B/T surgery. Experimental trauma model 2: critical-sized (4-mm) calvarial defects were created in $Tak1^{fl\text{-}frt/fl\text{-}frt}$ mice to assess TAK1 in bone healing with local injection of either (a) control adenovirus (Ad.control; 9×10^{10} plaque-forming unit (PFU) per injection site for 9 weeks); (b) Cre adenovirus (Ad.cre; 1.6×10^{11} PFU per injection site for 9 weeks), or (c) Cre/Flp (1×10^{10} PFU per injection site) virus (Ad.cre for every 3 days for 12 days followed by reconstitution of TAK1 expression with Ad.Flp for 8 weeks). Respective adenoviruses were injected into the calvarial defects.

In Vivo Drug Treatment: NG-25, TAK1 Inhibitor

C57BL/6 mice underwent burn/tenotomy as described above. Following injury mice received either phosphate-buffered saline vehicle control or TAK1 inhibitor (2 mg/kg) in 500 µl via intraperitoneal injection. Mice in both groups were euthanized at 3- and 9-weeks after injury for further analysis. Each group had $n \geq 3$ animals.

Cell Harvest

Mesenchymal cells, local tissue, and osteoblasts from $Tak1^{fl\text{-}frt/fl\text{-}frt}$, and corresponding littermate controls were harvested from (a) the inguinal fat pad (adipose-derived stem cells [ASCs]), (b) from the Achilles' tendon (tendon-derived cells; TdCs), and (c) from femur, tibia, and fibula (osteoblasts). All tissue was mechanically minced, digested with collagenase A and dispase. Cells were separated via 100 µm cell strainer and digestive enzyme were quenched in standard growth medium (Dulbecco's modified Eagle's medium [DMEM] supplemented with 10% fetal bovine serum [FBS] and 1% penicillin/streptomycin). Cells were spun down at 1,000 rpm for 5 minutes. The supernatant was discarded, and the cell pellet was resuspended in standard growth media and subsequently plated. Isolation of adipose and bone-marrow derived mesenchymal cells in this manner has previously been validated as demonstrating trilineage differentiation consistent with mesenchymal stem cells [36–39].

Cell Culture and Transfection

Cells were grown in standard growth medium (DMEM supplemented with 10% FBS and 1% penicillin/streptomycin). Cells used were all passage 2 through 6. $Tak1^{fl\text{-}frt/fl\text{-}frt}$ cells were treated with either Ad.LacZ (MOI 500), Ad. Cre (MOI 500) in DMEM free of FBS (serum deprived) for 24 hours. Cells were then cultured in standard growth media (serum-replete) for 48 hours. Subsequent transfection was then performed with either Ad.LacZ, Ad.Cre, or Ad. FLP (MOI 500). As with the initial transfection, second transfection was performed in DMEM free of FBS for 24 hours before being transitioned to standard growth media for 48 hours. At this point, cells were ready for RNA/protein harvest or for use in proliferation and differentiation assays.

Flow Cytometric Preparation and Confirmation of Purity

Adipose-derived stem cells were harvested as above and suspended in Hanks' balanced saline solution (HBSS) prior to filtration through a 70-µm sterile strainer and centrifuged at 800 rpm for 5 minutes before removing the supernatant and washing in HBSS. This process was repeated three times before incubation with fluorescently labeled antibodies. AmCyan viability dye used as a marker to gate for live versus dead cells. Lineage defined by the following myeloid markers CD45-PE; MHCII-PE; B220-PE; CD11b-FITC; CD34-FITC (eBioscience, Torrey Pines, CA; Thermo Fisher, Waltham, MA). Following 1 hour of incubation at 4°C, sample were washed and filtered through a 45-µm mesh filter before being run on a FACSAria II (BD Biosciences) Cell Sorter at the University of Michigan Flow Cytometry Core in the Biomedical Science Research Center. Samples were gated to separate debris and autofluorescent signals from the cell population. Data were then analyzed using the FlowJo Software (TreeStar). Flow cytometric data was normalized to account for differences in aggregate number between cell types.

siRNA Treatment. To generate TAK1 knockdown cells, ASCs and tendon-derived cells (TdCs) were transfected with siRNA (s77092, s77094, and negative control no. 1, Ambion) using Lipofectamine RNAiMAX transfection reagent (Thermo). For cell proliferation assays, siRNAs were transfected when cells were plated after 3–4 hours and the medium was changed. For cell differentiation assays, siRNAs were transfected when the medium was changed to osteogenic differentiation media (ODM) and every 2 days.

Proliferation Assays

Cells were seeded in 12-well plates at a density of 5×10^3 cells per well ($n = 3$). Cells were grown in standard growth medium

(DMEM supplemented with 10% FBS and 1% penicillin/streptomycin). Treatment groups had their media supplemented as follows: NG-25 (4 μM NG-25/DMSO in DMEM; 5Z-O) 1 μM 5Z-O/DMSO in DMEM. Media changed every 3 days. At 12, 24, 48, 72, and 96 or 144 hours cells were lifted following trypsin–EDTA treatment and were manually enumerated using trypan blue stain and a hemocytometer. Additionally, cell proliferation was assessed by bromodeoxyuridine (BrdU) incorporation.

Differentiation Assays

Cells were seeded in 12-well plates at a density of 3×10^3 cells per well ($n = 3$). Prior to differentiation cells were maintained in standard growth media (DMEM supplemented with 10% FBS and 1% penicillin/streptomycin). Differentiation was performed in ODM (DMEM supplemented with 10% FBS, 1% penicillin/streptomycin, 10 mM β-glycerophosphate, and 100 μg/ml ascorbic acid). ODM media in isolation was used for control groups. The NG-25 test group was treated with 4 μM NG-25/DMSO in ODM. Differentiation media were changed every 3 days. Cells for early RNA or protein quantification were collected after 3 days of differentiation. Early functional osteogenic differentiation was assessed by ALP stain and quantification of ALP enzymatic activity after 7 days. Alizarin red staining for bone mineral deposition and colorimetric quantification was completed at 14 days.

MicroCT Analysis

MicroCT scans (Siemens Inveon using 80 kVp, 80 mA, and 1,100-millisecond exposure) were used to quantify: HO volume in mice with burn/tenotomy. Images were reconstructed and HO volume quantified using a calibrated imaging protocol as previously described with the MicroView μCT viewer (Parallax Innovations, Ilderton, Canada) [14]. The calculation of the threshold for regenerating calvarial bone was performed in MicroView and determined equivalent to 800 Houndsfield Units. Percentage healing on the parietal bone containing the defect was determined by dividing the rest-defect area by the mean of the defect size at day 1 after surgery. TAK1 mice were scanned at 24 hours and 9 weeks after surgery.

Preparation of Tissue for Histology

Histologic evaluation was performed at indicated time points in hind limbs of burn/tenotomy mice (wild-type, *tmKO* and respective littermate controls) and calvarial defects of *Tak1*$^{fl\text{-}frt/fl\text{-}frt}$ mice. Hind limbs and calvaria were fixed in formalin overnight at 4°C and subsequently decalcified in 19% EDTA solution for 3–5 weeks at 4°C until x-ray verification of decalcification. Hind limbs were embedded in paraffin, and 5–7 μm sections were cut and mounted on Superfrost Plus slides (Fisherbrand, Hampton, NH) and stored at room temperature.

Histology and Immunostaining

Hematoxylin and eosin (H&E) and Movat's pentachrome staining were performed of the ankle region and calvaria, respectively. Immunostaining of extraskeletal ectopic bone was performed on rehydrated wax sections with the following primary antibodies: rabbit anti-PDGFR (antibody sc-338, Santa Cruz Biotechnology, Dallas, TX), mouse anti-PDGFR (antibody sc-398206, Santa Cruz Biotechnology) goat anti-Sox9 (antibody sc-17341, Santa Cruz Biotechnology), rabbit anti-Ki67 (antibody AB9260, Millipore, Darmstadt, Germany), goat anti-mouse anti-pSmad1/5 (antibody sc-12353, Santa Cruz Biotechnology), polyclonal rabbit anti-TAK1 (NB100-56363, Novus Biologicals, Littleton, CO), rabbit anti-pTAK1 (antibody sc-4508, Cell Signaling, Danvers, MA), goat anti-pSmad1/5/8 (antibody sc-12353, Santa Cruz Biotechnology), rabbit anti-pSmad 2/3 (antibody sc-11769 Santa Cruz Biotechnology), rabbit anti-pTAK1 (antibody NBP1-9609, Novus Biologicals, Littleton, CO), rabbit anti-pp38 (antibody sc-9211, Cell Signaling). Appropriate dilutions were determined before achieving final images. The appropriate fluorescent secondary antibody was applied and visualized using fluorescent microscopy. Secondary antibodies consisted of anti-rabbit or anti-goat Alexafluor-488 (green) or Alexafluor-594 (red; A21206, A11055, A21207, A11058, Life Technologies).

Quantification of Calvarial Defect Healing

Histomorphometric measurements to quantify the area of regenerate bone were performed using ImageJ on every 10th Aniline Blue stained slide of the defect (Ad.LacZ: six defects, 118 total images; Ad.Cre: six defects, 120 total images; Ad.Cre/Ad.Flp: eight defects, 120 total images). Regenerative bone was manually selected and isolated from each section and the area calculated using the measure function on ImageJ. For each defect, measured areas were summed to estimate total new bone formation.

Microscopy

All fluorescently stained images were taken using an Olympus BX-51 upright light microscope equipped with standard DAPI, 488 nm, and TRITC cubes attached to an Olympus DP-70 high resolution digital camera. Each site was imaged in all channels and overlaid in DPViewer before examination in Adobe Photoshop. H&E, safranin O, pentachrome, and aniline blue sections were imaged at ×10 and ×20 magnification. Immunofluorescent images were taken at either ×20 or ×40 magnification. Immunocytochemical images were taken at ×60 and ×100 magnification under oil. Scale bars were placed for all images with a standard 200 μm diameter.

Western Blot Analysis

Tissue/cells were lysed with RIPA lysis buffer (Santa Cruz Biotechnology) containing protease inhibitors, 1 nM sodium orthovanadate, 1 mM PMSF. The protein concentration was determined using the BCA Plus protein assay kit (Pierce, Rockford, IL). SDS-PAGE was used to separate the protein extract (40 μg). After transfer to a polyvinylidene fluoride membrane (EMD, Millipore, Darmstadt Germany), and blocking with 5% milk in TBS with 0.1% Tween-20 (TBST) for 1 hour, then incubated overnight with the following antibodies at 4°C: rabbit anti-pTak1 (antibody sc-9339, Cell Signaling), rabbit anti-TAK1 (NB100-56363, Novus Biologicals, Littleton, CO), rabbit anti-pSmad1/5/8 (antibody 9516, Cell Signaling), rabbit anti-Smad2/3 (antibody sc-3102, Cell Signaling), rabbit anti-pp38 (antibody 9211, Cell Signaling), rabbit anti-PCNA (antibody 2586, Cell Signaling), and rabbit anti-α-tubulin (antibody 2144, Cell Signaling). After washing with TBST five times, the membrane was incubated with appropriate Horseradish peroxidase (HRP)-conjugated secondary antibody (antibody 7074, Cell Signaling) for 30 minutes at room temperature and detected using chemiluminescence PICO substrate (Pierce, Rockford, IL).

Gene Analysis

To assess the recombination efficiency of the floxed Tak1 locus (exon 2) and gene expression in the total RNAs were isolated from AdMSCs transfected with Ad.LacZ, Ad.Cre, Ad.FLP, and Ad.Cre/Ad.

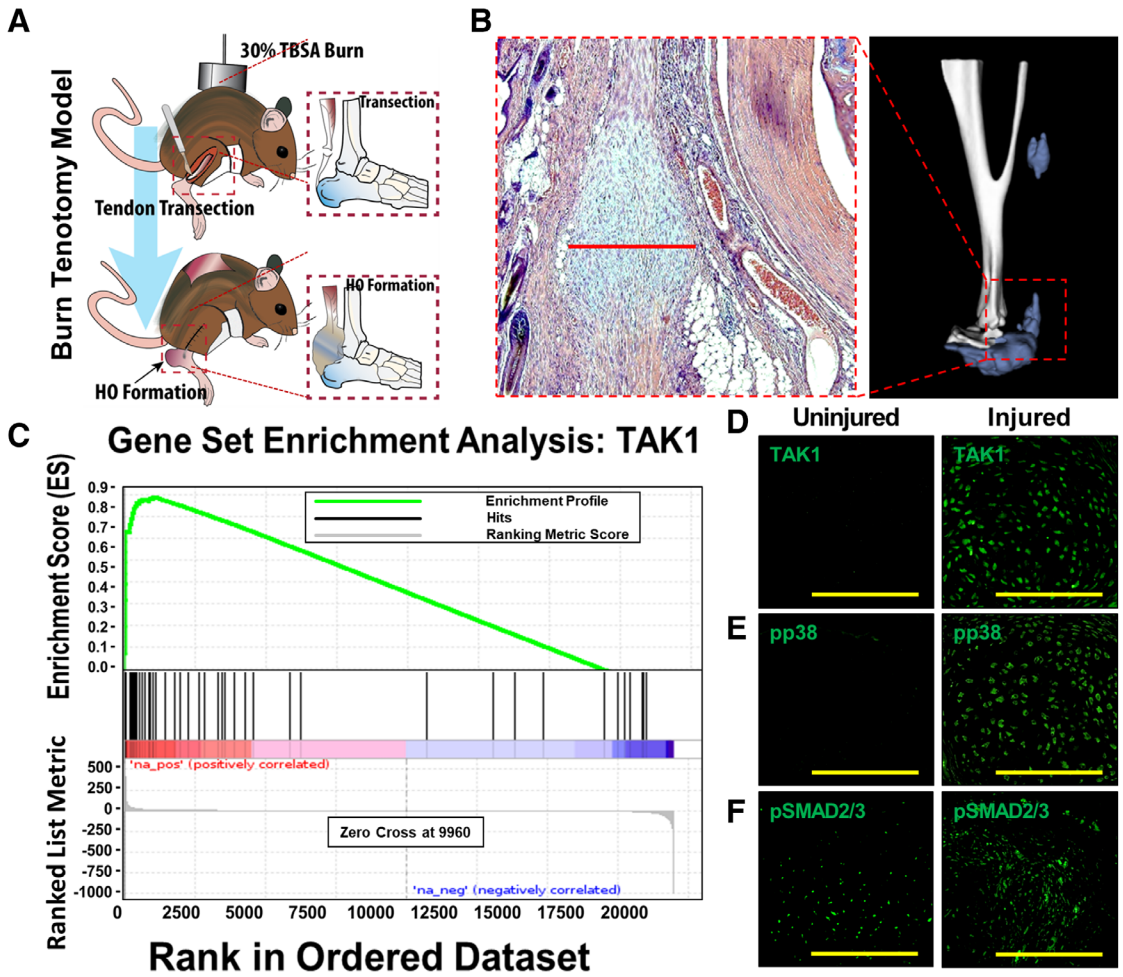

Figure 1. Transforming growth factor-β activated kinase 1 (TAK1) signaling mediates pathologic wound healing after musculoskeletal injury. **(A):** Mouse model of musculoskeletal injury with hind limb tenotomy and dorsal 30% total body surface area burn injury—tenotomy at midpoint of Achilles' tendon; burn ipsilateral to tenotomy. Histologic sections are collected from region between tibial midpoint and calcaneus at the site of highest chondrogenic and osteogenic differentiation. **(B):** Representative three-dimensional reconstruction (9 weeks) and H&E (3 weeks) demonstrating localization of heterotopic ossification. **(C):** Gene set enrichment analysis demonstrates upregulation of TAK1 signaling at the tendon transection site 3 weeks after injury (Enrichment Score = 0.88, FDR < 0.001). **(D):** Expression of TAK1 in the uninjured and injured hind limb—expression of TAK1 highest at areas undergoing early chondrogenic differentiation. **(E):** Expression of pp38 in the uninjured and injured hind limb—expression of pp38 highest in area undergoing early chondrogenic differentiation. **(F):** Expression of pSMAD2/3 in the uninjured and injured hind limb—expression of pSMAD2/3 highest in areas of mesenchymal condensation adjacent to areas of chondrogenic differentiation. Histology at 3 weeks after injury; ×40 magnification. Scale bars = 200 μm.

FLP (RNeasy Mini Kit; Qiagen, Germantown, MD) per manufacturer's specifications, and 1 μg RNA using High capacity cDNA reverse transcription kit (Applied Biosystems, Foster City, CA) according to manufacturer's protocols. Quantitative real-time PCR was carried out using the Applied Biosystems Prism 7900HT Sequence Detection System and SybrGreen PCR Master Mix (Applied Biosystems, Beverly, MA). Specific primers for these genes were:

Tak1 Forward: GGTTGTCGGAAGAGGAGCTTTT
Tak1 Reverse: AACTGCCGGAGCTCCACAAT
Gapdh Forward: TCTCCTGCGACTTCAACAGCAA
Gapdh Reverse: CCCACATACCAGGAAATGAGCTTG
Alp Forward: TCTGCCTTGCCTGTATCTGGAATC
Alp Reverse: GTGCTTTGGGAATCTGTGCAGTCT
Runx2 Forward: CACCGAGACCAACCGAGTCATTTA
Runx2 Reverse: AAGAGGCTGTTTGACGCCATAG
Sox9 Forward: GGAGGAAGTCGGTGAAGAAC
Sox9 Reverse: AGCGCCTTGAAGATAGCATT

The PCR protocol included a 95°C denaturation (20 seconds), annealing (20 seconds), and 72°C extension (30 seconds). Detection of the fluorescent product was carried out at the end of the 72°C extension period. Each sample was tested at least in triplicate and repeated for three independent cell/tissue preparations.

Statistical Analysis

Means and SDs were calculated from numerical data, as presented in the text, figures, and figure legends. In figures, bar graphs represent mean, whereas error bars represent 1 SD. Statistical analysis was performed using a Student's *t* test to directly compare two groups. *p*-Values are included in figure legends.

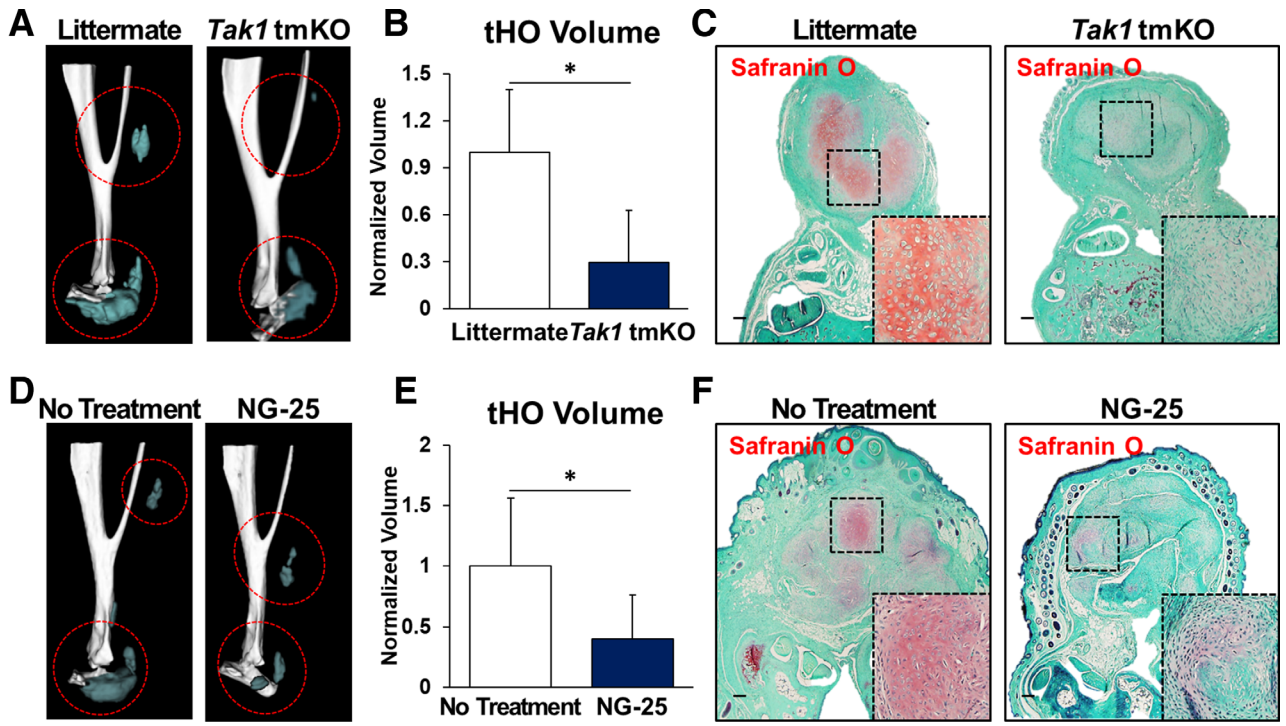

Figure 2. Transforming growth factor-β activated kinase 1 (TAK1) signaling is associated with heterotopic ossification after musculoskeletal injury. **(A):** Three-dimensional (3D) microCT reconstruction of Tak1 tmKO (tamoxifen-inducible postnatal Tak1 knockout [Tak1tmKO: Ub.CreERT/Tak1$^{fx\text{-}frt/fx\text{-}frt}$]) and littermate control hind limbs showing heterotopic bone 9 weeks after injury (red circles around heterotopic ossification), tamoxifen was injected 7 and 3 days before injury and 3 days after injury. **(B):** Quantification of heterotopic bone volume in Tak1 tmKO and littermate control hind limbs showing heterotopic bone 9 weeks after injury (1.0 versus 0.29, $p < .05$); **(C):** Safranin O staining (red stain) in Tak1 tmKO and littermate control hind limbs showing cartilage 3 weeks after injury (×4 magnification; dotted box indicates site of magnified image in right bottom corner). **(D):** 3D microCT reconstruction of NG-25 and treatment control hind limbs showing heterotopic bone 9 weeks after injury. **(E):** Quantification of heterotopic bone volume in NG-25 and treatment control hind limbs showing heterotopic bone 9 weeks after injury (1.0 versus 0.35, $p < .05$). **(F):** Safranin O staining (red) in NG-25 and treatment control hind limbs showing cartilage 3 weeks after injury (×4 magnification; dotted box indicates site of magnified image in right bottom corner). All scale bars = 200 μm; $n \geq 5$ for all quantifications; *, $p < .05$.

RESULTS

TAK1 Signaling Mediates Pathologic Wound Healing After Musculoskeletal Injury

To study aberrant wound healing, we used a model of tHO consisting of hind limb Achilles' tendon transection with dorsal burn injury (Fig. 1A, 1B) [16]. Gene set enrichment analysis of RNA sequencing data from hind limb tissue samples obtained from mice 3 weeks after injury identified upregulation of the TAK1 pathway when compared with the uninjured hind limb (Enrichment Score [ES] = 0.88, False discovery rate (FDR) < 0.001; Fig. 1C). Immunostaining also confirmed upregulation of TAK1 protein expression at the injury site 3 weeks after injury (Fig. 1D), and importantly upregulation of phosphorylated proteins downstream in the TAK1 pathway including pp38 and pSMAD 2/3 (Fig. 1E, 1F). Previous studies have shown that TAK1, an intracellular mediator of TGF-β and BMP signaling, plays a key role in normal postnatal endochondral ossification [24–26], making it a potential target to eliminate HO.

We first developed a mouse allowing targeted deactivation and reactivation of *Tak1* (Tak$^{fx\text{-}frt/fx\text{-}frt}$; Supporting Information Fig. S2) and confirmed that genetic loss of *Tak1* by tamoxifen inducible Ubiqutin-CreER (Ub.CreERT) significantly reduces tHO radiographically and histologically (Fig. 2A, 2C; Supporting Information Fig. S3A). Systemic treatment of wild-type mice with NG-25, a TAK1 inhibitor, which occupies the ATP binding pocket of TAK1 [33], significantly reduced tHO volume (Fig. 2D, 2E; Supporting Information Fig. S3B) and decreased cartilage presence 3 weeks after injury (Fig. 2F). Correspondingly, treatment with NG-25 reduced pSMAD 1/5, pSMAD 2/3, and SOX9 expression on immunostaining (Supporting Information Fig. S4A–S4C). These findings indicate that genetic or pharmacologic loss of TAK1 reduced pathologic wound healing, providing a novel target for therapeutic intervention.

Genetic Loss of Tak1 Within Mesenchymal Cells Alters Cellular Proliferation and Differentiation to Prevent tHO

We have previously shown that Prx-Cre expressing cells, mesenchymal progenitors, contribute to tHO [14] induced by hind limb Achilles' tendon transection with dorsal burn injury. Because immunostaining of tissue from the injury site indicated that TAK1 signaling is present in MSCs (Fig. 3A) we generated a *Tak1* conditional knockout mouse for MSCs (*Tak1* cKO; *Prxcre/Tak1*$^{fx\text{-}frt/fx\text{-}frt}$). Histologic analysis demonstrated little-to-no evidence of cartilage, compared with our Wild Type (WT) control (Fig. 3B). Immunostaining confirmed reduction of pTAK1 at the injury site of these mice (Fig. 3C). Interestingly, when compared with littermate controls, Tak1 cKO mice had increased cellular proportion of K67+ cells at the injury site (Fig. 3D).

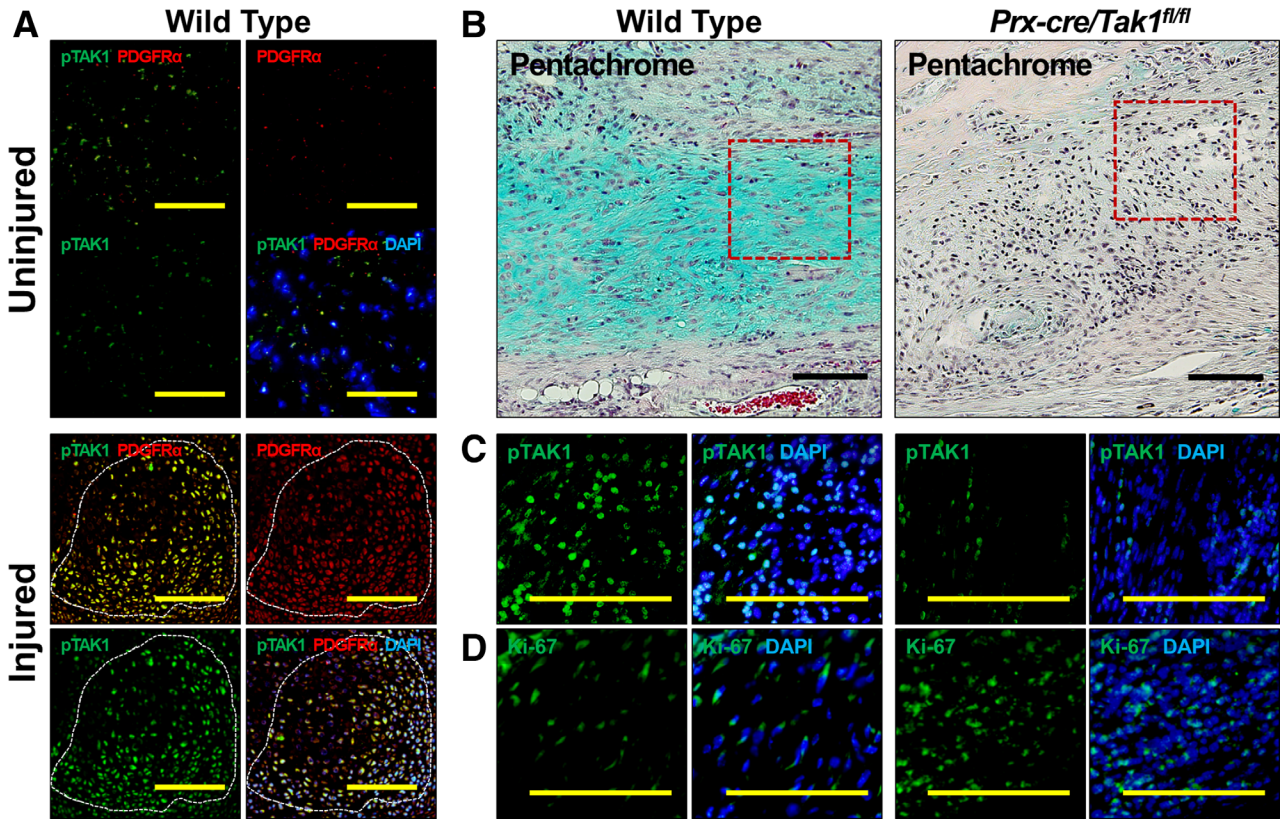

Figure 3. Genetic loss of transforming growth factor-β activated kinase 1 (TAK1) signaling in mesenchymal cells increases cell proliferation and impairs chondrogenic differentiation to prevent trauma-induced heterotopic ossification. **(A):** Coexpression of pTAK1 and PDGFRα+ in the injured and uninjured hind limb 3 weeks after injury (×20 magnification; top left corner: pTAK1—*green* overlay with PDGFRα—*red*; bottom right corner: pTAK1—*green* overlay with PDGFRα—*red* and DAPI—*blue*). **(B):** Pentachrome of injury site of Prx-cre/Tak1$^{fx\text{-}frt/fx\text{-}frt}$ and littermate control mice 3 weeks after injury (×10 magnification; Alcian blue represents cartilaginous tissue; red box shows areas of immunostaining). **(C):** Immunostaining for pTAK1 at the injury site of Prx-cre/Tak1$^{fx\text{-}frt/fx\text{-}frt}$ and littermate control mice 3 weeks after injury (×10 magnification; right side: pTAK1—*green* overlay with DAPI—*blue*). **(D):** Immunostaining for Ki67 at the injury site of Prx-cre/Tak1$^{fx\text{-}frt/fx\text{-}frt}$ and littermate control mice 3 weeks after injury (×10 magnification; right side: Ki67—*green* overlay with DAPI—*blue*). All scale bars = 200 μm.

Consistent with these findings and previously published results, MSCs isolated from adipose tissues of *Tak1*$^{fx\text{-}frt/fx\text{-}frt}$ mice (Supporting Information Fig. S5A–S5C) exhibited markedly reduced in vitro osteogenic and chondrogenic differentiation upon treatment with adenovirus Cre (Ad.Cre) when compared with adenovirus control (Ad.LacZ; Supporting Information Fig. S6A–S6E). Additionally, *Tak1*$^{fx\text{-}frt/fx\text{-}frt}$ MSCs treated with Ad.Cre exhibited increased proliferation when compared with *Tak1*$^{fx\text{-}frt/fx\text{-}frt}$ MSCs treated with Ad.LacZ (Fig. 4A, 4B). NG-25 also reduced osteogenic differentiation and chondrogenic differentiation of MSCs in vitro (Supporting Information Fig. S7A–S7F). In contrast, NG-25-treated MSCs demonstrated reduced proliferation when compared with vehicle control-treated cells (Fig. 4C, 4D). Similarly, 5Z-7-oxozeaenol (5Z-O) [33], a potent ATP competitive irreversible inhibitor of TAK1 significantly reduced proliferation when compared with vehicle control-treated cells (Supporting Information Fig. S8A, S8B). The reduction in cell proliferation observed with currently developed TAK1 inhibitors may be due to their off target effects including inhibition of Abelson tyrosine kinase (ABL), an essential molecule that regulates cell proliferation [33]. To test this, we developed a system to silence *Tak1* with multiple siRNAs (Fig. 4E; Supporting Information Fig. S9A, S9B). Utilizing these specific siRNAs we found a similar increase in cell proliferation by BrdU assay and cell counting (Fig. 4F, 4G). Treatment with siRNA, similar to *Tak1* knockout with our mouse model, decreased in vitro osteogenic differentiation by alkaline phosphatase (ALP) and alizarin red (Fig. 4H). Overall, these findings suggest that current pharmacologic inhibitors of TAK1 are unable to phenocopy genetic loss of *Tak1* in the setting of tissue injury, indicating the need for more specific TAK1 inhibitors.

In Vitro Validation of a Novel Dual-Inducible Model to Knockout and Rescue Tak1 Signaling Using COSIEN

The important finding that loss of Tak1 upregulates proliferation led us to consider whether this property can be used to improve tissue regeneration. Typically, studies using pharmacologic agents to improve tissue regeneration have focused on the effects of these mediators during the "drug on" period. Interestingly, implicit in studies evaluating regenerative therapies is a period during which drug is not present within the organism—this "drug off" period may be in between doses or following completion of agent administration. The role of the "drug off" period, which proliferating cells may be able to undergo differentiation, has gone largely unrecognized in tissue regeneration. Therefore, because TAK1 is required for

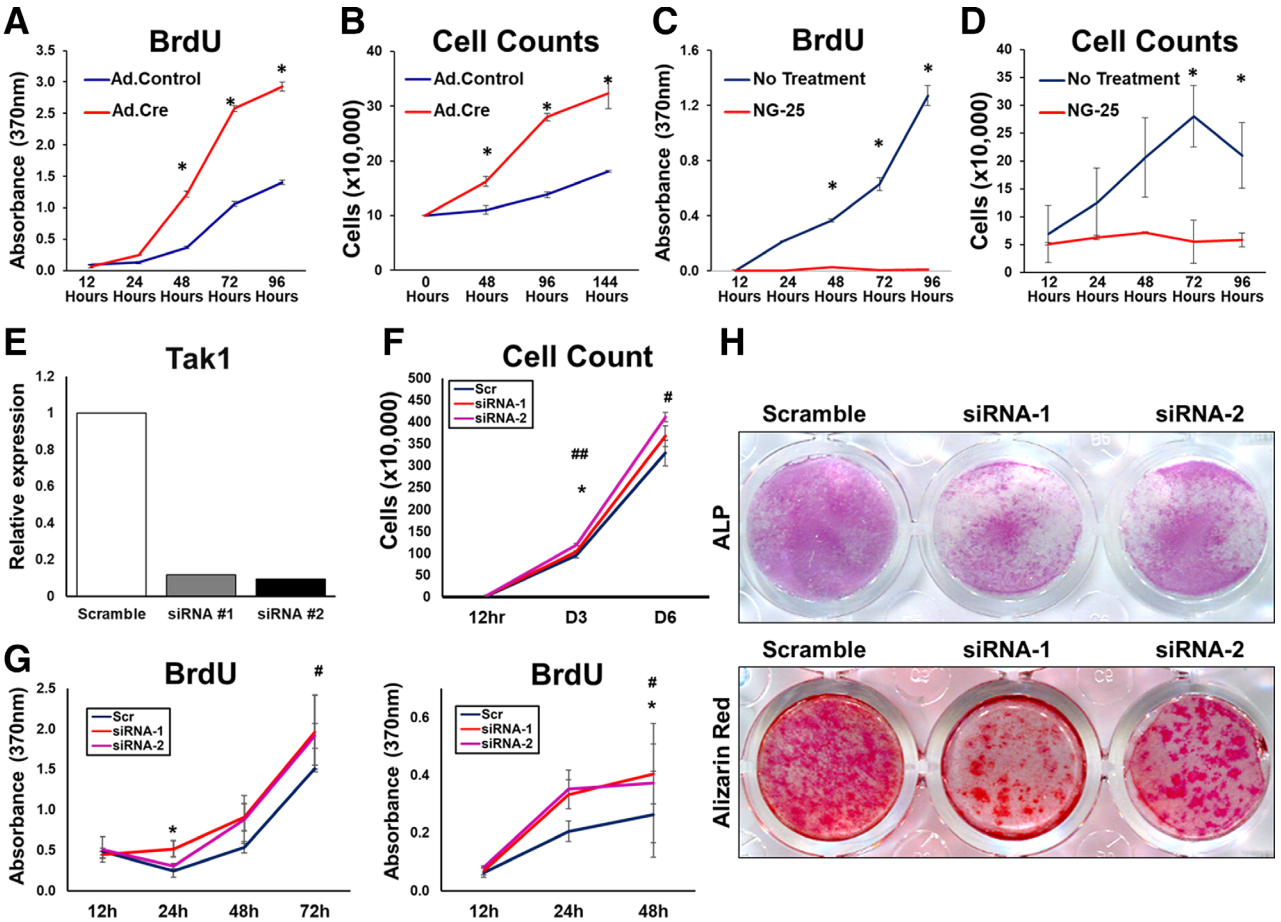

Figure 4. Comparison of pharmacologic and genetic transforming growth factor-β activated kinase 1 (TAK1) inhibition. **(A):** Cell proliferation (BrDU) of Ad.Cre and Ad.LacZ treated Tak1$^{fx\text{-}frt/fx\text{-}frt}$ adipose-derived stem cells (ASCs). **(B):** Cell proliferation (cell counting) of Ad.Cre and Ad.LacZ treated Tak1$^{fx\text{-}frt/fx\text{-}frt}$ ASCs. **(C):** Cell proliferation (BrDU) of ASCs treated with NG-25. **(D):** Cell proliferation (cell counting) of ASCs treated with NG-25. **(E):** ASCs were transfected with siRNAs for TAK1, and TAK1 expression level was analyzed by qPCR. **(F):** Cell counting showing that siRNAs for TAK1 transfection significantly promote cell proliferation in vitro. **(G):** BrDU proliferation assay showing that siRNAs for TAK1 transfection significantly promote cell proliferation in vitro (left: ASCs and right: tendon-derived cells [TdCs]). **(H):** Osteoblastic differentiation assay showing that siRNAs for TAK1 transfection significantly suppressed the differentiation in vitro (upper: ALP stained TdCs at day 5 and lower: alizarin red stained TdCs at day 12). *, $^{\#}$, $p < .05$; $^{\#\#}$, $p < .01$. Student's *t* test (*, scramble versus siRNA-1; $^{\#}$, scramble versus siRNA-2).

cell differentiation and extracellular matrix (ECM) production [23, 24, 26], we sought to determine whether TAK1 could be modulated to improve regeneration of tissues through a coordinated approach of TAK1 inhibition (proliferation) and subsequent reactivation (differentiation).

Based on our findings, we determined that current pharmacologic inhibitors of TAK1, like many pathway directed therapies, are not specific enough to provide insight into a "drug on"/"drug off" strategy to improve tissue healing. We decided to mimic this approach taking advantage of an important design aspect of the *Tak1*$^{fx\text{-}frt/fx\text{-}frt}$ mouse—in particular, this is a novel *dual* inducible Cre/Flp mouse model allowing for loss of gene function (Cre/lox) followed by rescue (Flp/Frt). We have named this the COSIEN mouse, as the targeted gene segment is initially inverted or "gene off" by Cre and then subsequently reinverted or "gene on" by Flp. Mutations were introduced into the Lox and Frt recognition sites to allow only one-time inversion (Cre) and reversion (Flp) of the targeted gene segment (Fig. 5A). This model was then validated genotypically in live animals (Supporting Information Fig. S10A–S10D). Although dual inducible models have been reported before to control temporal knockout of separate genes in neural development and tumor models [34–36], to the best of our knowledge, use of a dual inducible approach to inactivate and subsequently reactivate gene activity has not been described. This ability to optimize gene disruption and reactivation in a timed fashion would allow therapeutic optimization for developmental and post-traumatic pathologies.

MSCs isolated from *Tak1*$^{fx\text{-}frt/fx\text{-}frt}$ mice showed reduced *Tak1* mRNA expression with Ad.Cre, which was subsequently rescued after Ad.Flp treatment (Fig. 5B). Protein level expression of pTAK1, pp38, pSMAD 1/5, and pSMAD 2/3 were reduced with Ad.Cre but increased with subsequent Ad.Flp treatment (Ad.Cre/Ad.Flp; Fig. 5C–5G). As expected, genetic loss of *Tak1* (Ad.Cre) reduced osteogenic differentiation while subsequent rescue of *Tak1* (Ad.Cre/Ad.Flp) improved osteogenic differentiation relative to Ad.LacZ treatment (Supporting Information Fig. S11A, S11B). Taken together, these findings confirm that the COSIEN mouse provides an approach to study "drug on" (Ad.Cre) and "drug off" (Ad.Flp) with specificity for *Tak1.*

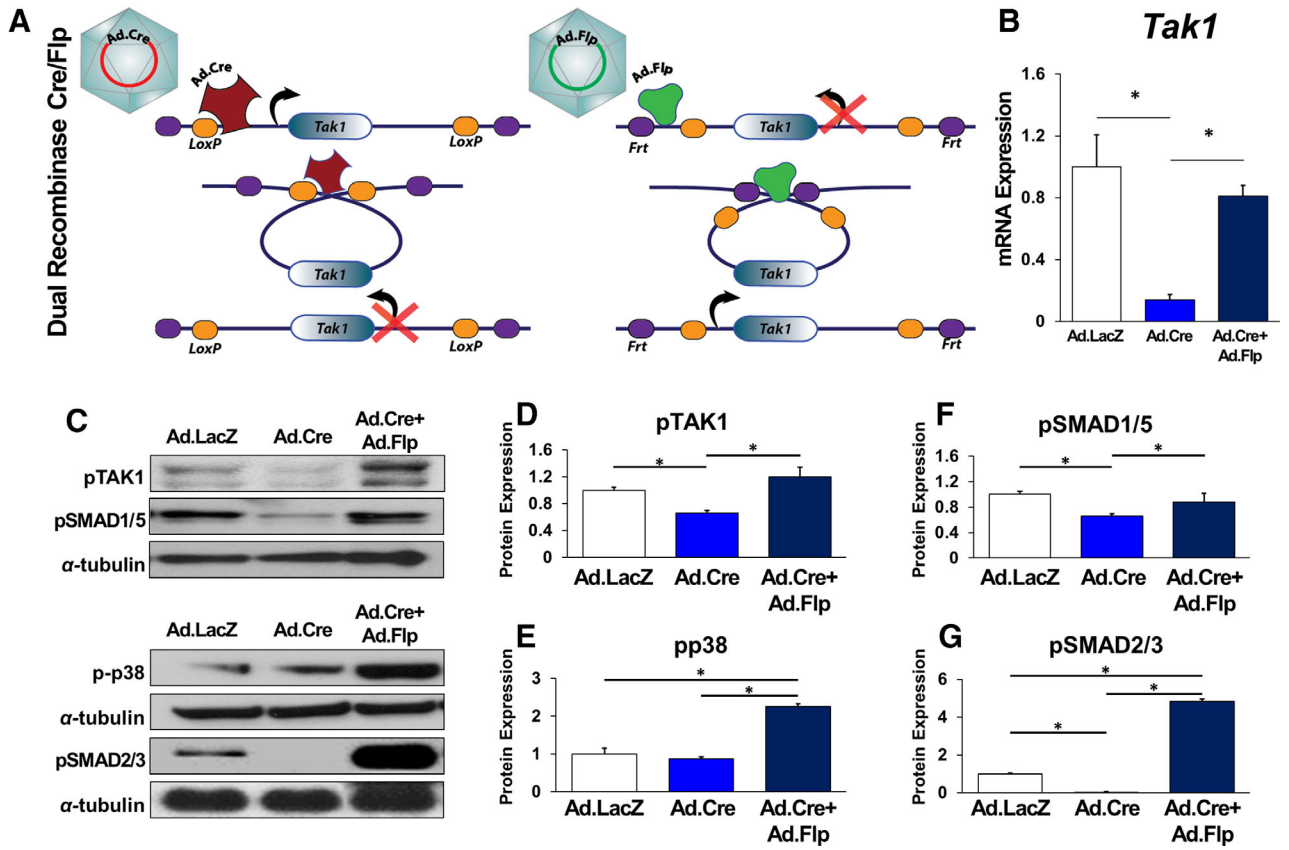

Figure 5. In vitro validation of a dual-inducible model to knockout and rescue transforming growth factor-β activated kinase 1 (TAK1) signaling using COmbinational Sequential Inversion ENgineering. **(A):** Schematic for dual-inducible model within the Tak1$^{fx\text{-}frt/fx\text{-}frt}$ mouse: mutations are introduced into the Lox and Frt sites to allow only one-time inversion and reversion of the targeted gene segment. Initial inversion (*loss of gene function*) is driven by a Cre/Lox system following addition of Ad.Cre. Rescue reversion (*return of gene function*) is driven by a Flp/Frt system following addition of Ad.Flp. **(B):** Normalized quantification of Tak1 gene expression from Ad.LacZ, Ad.Cre, and Ad.Cre + Ad.Flp treated mesenchymal cells (Ad.LacZ: 1.0; Ad.Cre: 0.41; Ad.Cre + Ad.Flp: 0.55). **(C):** Representative immunoblot of Ad.LacZ, Ad.Cre, and Ad.Cre + Ad.Flp treated mesenchymal cells for pTAK1, pSMAD 1/5, pp38, pSMAD 2/3, and α-tubulin. **(D):** Normalized quantification of pTAK1 protein expression from Ad.LacZ, Ad.Cre, and Ad.Cre + Ad.Flp treated mesenchymal cells (Ad.LacZ: 1.0; Ad.Cre: 0.66; Ad.Cre + Ad.Flp: 1.2). **(E):** Normalized quantification of pp38 protein expression from Ad.LacZ, Ad.Cre, and Ad.Cre + Ad.Flp treated mesenchymal cells (Ad.LacZ: 1.0; Ad.Cre: 0.65; Ad.Cre + Ad.Flp: 0.88). **(F):** Normalized quantification of pSMAD1/5 protein expression from Ad.LacZ, Ad.Cre, and Ad.Cre + Ad.Flp treated mesenchymal cells (Ad.LacZ: 1.0; Ad.Cre: 0.87; Ad.Cre + Ad.Flp: 2.25). **(G):** Normalized quantification of pSMAD 2/3 protein expression from Ad. LacZ, Ad.Cre, and Ad.Cre + Ad.Flp treated mesenchymal cells (Ad.LacZ: 1.0; Ad.Cre: 0.02; Ad.Cre + Ad.Flp: 4.81). All cells were treated with Ad.Cre (or Ad.LacZ) for 24 hours under serum deprivation conditions followed by 48 hours in serum replete and subsequently treated with Ad.LacZ (Ad.LacZ group), Ad.Cre (Ad.Cre group), or Ad.Flp (Ad.Cre + Ad.Flp) for 24 hours in serum deprived conditions followed by culture for an additional 2 days in serum replete conditions. Mesenchymal cells described are adipose-derived stem cells; *, $p < .05$.

Improved Bone Regeneration with Dual-Inducible Model to Evaluate "Drug on" and "Drug off" Therapeutic Strategy Targeting TAK1

After validating the COSIEN model in vitro, we next studied its effect in vivo using a critical-size calvarial defect model. Calvarial defects are often used for the study of bone healing; although most studies describing critical-size calvarial defects use scaffolds impregnated with MSCs or growth factors, these approaches may be difficult to translate clinically. To validate the COSIEN model in vivo and to demonstrate that a regenerative medicine strategy emphasizing both the "drug on" and "drug off" periods of therapy could improve wound healing, we injected mice with either Ad.LacZ only, Ad.Cre only, or Ad.Cre followed by Ad.Flp (Ad.Cre/Ad.Flp), directly into the calvarial defect area for 9 weeks (Fig. 6A). For the third regimen, Ad.Flp was started to inject from the second week. As expected, mice treated with Ad.Cre/Ad.Flp had significantly more osteoid deposition on the basis of microCT (Fig. 6B) and histologically with aniline blue quantification (Fig. 6C, 6D). The Ad.Cre group developed similar amount of tissues with the Ad/Cre/Ad.Flp group, but osteoid formation remained similar to the control group (Fig. 6C, 6D). Calvarial samples obtained from *Tak1*$^{fx\text{-}frt/fx\text{-}frt}$ mice showed reduced *Tak1* mRNA expression with Ad.Cre, which was subsequently restored after Ad.Flp treatment (Fig. 6E).

Levels of pTAK1, pSMAD 1/5, and pSMAD 2/3 from these samples were found reduced in the Ad.Cre group but increased with subsequent Ad.Flp treatment (Ad.Cre/Ad.Flp group; Fig. 7A–7D). Immunostaining confirmed a decrease of TAK1 (Ad.Cre) with subsequent rescue of TAK1 (Ad.Cre/Ad.Flp; Fig. 7E) and also increased presence of MSCs (PDGFRα+) in both the Ad.Cre and Ad.Cre/Ad.Flp groups (Fig. 7F). Immunostaining for pSMAD2/3 was consistent with immunoblot results (Supporting Information Fig. S12). Proliferation observed by Ki67 was increased in the Ad.Cre versus Ad.LacZ group, with restoration of normal pattern on Ad.Flp administration (Fig. 7G). This was confirmed

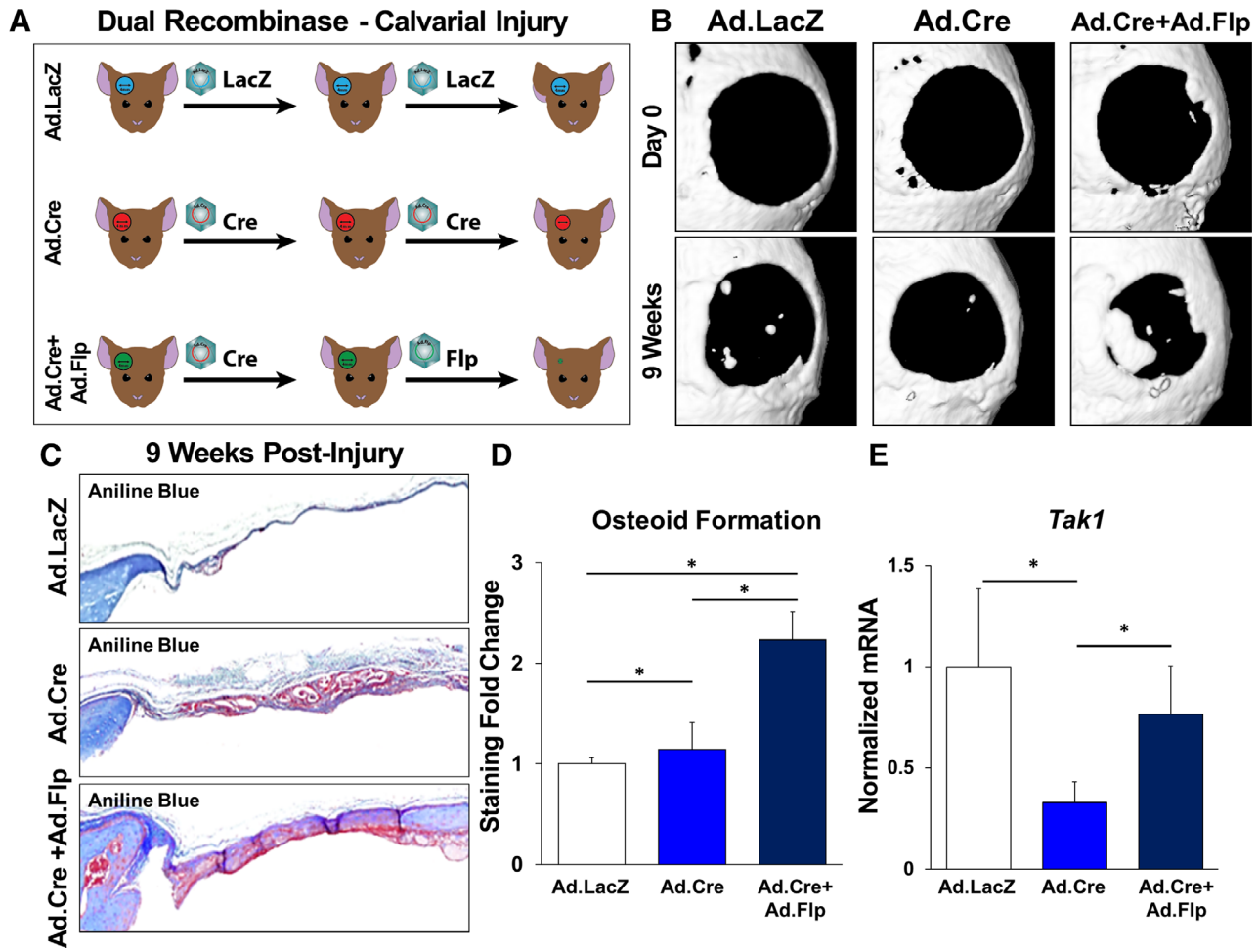

Figure 6. Improved regeneration with Cre/Flp dual inducible mouse model to simulate "drug on" and "drug off" therapeutic strategy targeting transforming growth factor-β activated kinase 1 (TAK1) signaling. **(A):** Calvarial defect schematic with Ad.LacZ, Ad.Cre, or Ad.Cre/Ad.Flp. **(B):** Representative microCT scans showing healing of Ad.LacZ, Ad.Cre, and Ad.Cre/Ad.Flp treated calvarial defects at 9 weeks with corresponding baseline scans at day 1. **(C):** Representative aniline blue staining of the calvarial defect site 9 weeks after injury (dashed black box marks defect site). **(D):** Normalized quantification of osteoid in Ad.LacZ, Ad.Cre, and Ad.Cre/Ad.Flp treated calvarial defects 9 weeks after injury (Ad.LacZ: 1.0; Ad.Cre: 1.14; Ad.Cre/Ad.Flp: 2.23). **(E):** Normalized quantification of Tak1 gene expression from Ad.LacZ, Ad.Cre, and Ad.Cre/Ad.Flp treated calvarial defects (Ad.LacZ: 1.0; Ad.Cre: 0.33; Ad.Cre/Ad.Flp: 0.76). In experimental groups, defects were treated with Ad.Cre every 3 days starting from the day of surgery until day 12; at day 12, defects were treated with either Ad.Cre (Ad.Cre group) or Ad.Flp (Ad.Cre/Ad.Flp group); in control group, defects were treated with Ad.LacZ every 3 days. Cells for protein extraction collected by harvest of the calvarial defect after removal of dura; *, $p < .05$.

with immunoblotting for PCNA in protein obtained from Ad.LacZ, Ad.Cre, and Ad.Cre/Ad.Flp treated calvaria (Supporting Information Fig. S13A, S13B).

Discussion

tHO is a clinical phenomenon which occurs in patients following severe trauma, and is characterized by the development of extraskeletal bone in soft tissues. Our findings indicate that TAK1 can be targeted pharmacologically to prevent tHO. We then use this model of pathologic wound healing to elucidate a critical aspect of therapeutic regimens—the contribution of the "drug on" and the "drug off" state to therapeutic impact. Taken together, our findings using the COSIEN mouse (*Tak1*$^{fx\text{-}frt/fx\text{-}frt}$) suggest that a coordinated "drug on" and "drug off" strategy may be critical for pharmacologic improvement of tissue regeneration, thereby transforming the paradigm of regenerative medicine. Although current studies focus primarily on the "drug on" state, implicit in these treatment strategies is a "drug off" state, which also contributes to healing. The dual inducible approach may allow for validation of gene targets considering both the "drug on" and "drug off" effects prior to pharmacologic development in the context of wound healing.

Patients with tHO are faced with debilitating pain, nonhealing wounds, and joint contractures limiting function [17, 18, 37]. We have previously shown that tHO forms via endochondral ossification, and that inhibition of hypoxic signaling reduces tHO through its effects on cartilage production [14]. We focused on TAK1 signaling due to the prominent role of TGF-β signaling during normal cartilage development [20–26]. Mice with genetic loss of *Tak1* driven by the Col2 or Prx promoters (Col2-cre or Prx-cre) exhibit impaired cartilage formation and loss of secondary ossification centers [25]. In this study, we found that mice with tamoxifen-inducible systemic loss of Tak1 exhibit

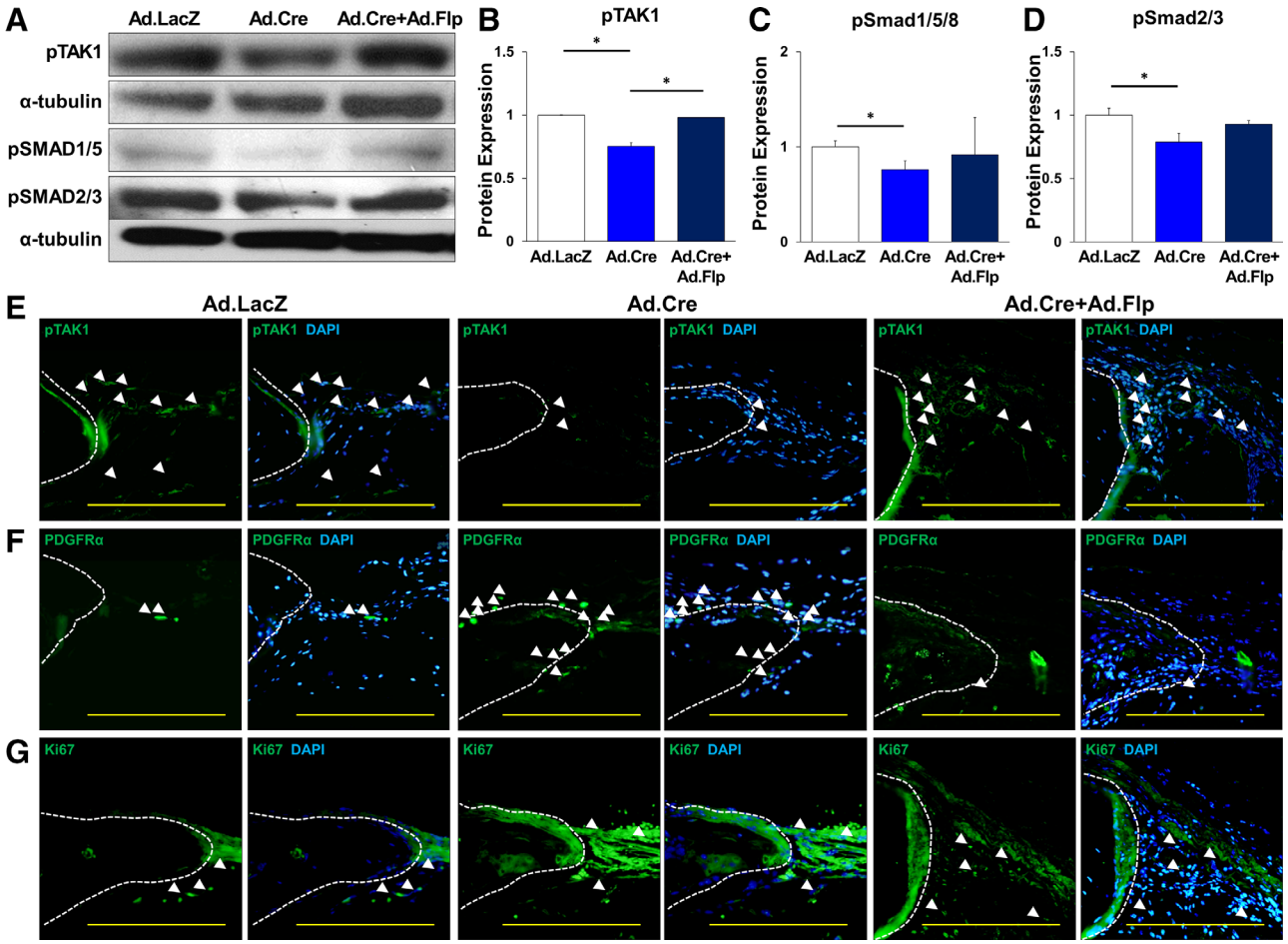

Figure 7. Increased cellular proliferation during transforming growth factor-β activated kinase 1 (TAK1) inactivation followed by differentiation during Tak1 reactivation. **(A):** Representative immunoblot of Ad.LacZ, Ad.Cre, and Ad.Cre/Ad.Flp treated calvarial defects for pTAK1, pSMAD 1/5, pSMAD 2/3, and α-tubulin. **(B):** Normalized quantification of pTAK1 protein expression from Ad.LacZ, Ad.Cre, and Ad.Cre/Ad.Flp treated calvarial defects (Ad.LacZ: 1.0; Ad.Cre: 0.75; Ad.Cre/Ad.Flp:0.98). **(C):** Normalized quantification of pSMAD 1/5 protein expression from Ad.LacZ, Ad.Cre, and Ad.Cre/Ad.Flp treated calvarial defects (Ad.LacZ: 1.0; Ad.Cre: 0.82; Ad.Cre/Ad.Flp: 1.43). **(D):** Normalized quantification of pSMAD 2/3 protein expression from Ad.LacZ, Ad.Cre, and Ad.Cre/Ad.Flp treated calvarial defects (Ad.LacZ: 1.0; Ad.Cre: 0.82; Ad.Cre/Ad.Flp: 1.43). **(E):** Representative immunostaining of Ad.LacZ, Ad.Cre, and Ad.Cre/Ad.Flp treated calvarial defects for pTAK1. **(F):** Representative immunostaining for PDGFRα in Ad.LacZ, Ad.Cre, Ad.Cre/Ad.Flp treated calvarial defects 9 weeks after injury. **(G):** Representative immunostaining for Ki67 in Ad.LacZ, Ad.Cre, Ad.Cre/Ad.Flp treated calvarial defects 9 weeks after injury. White dotted line marks edge of native calvaria. Cells for protein extraction collected by harvest of the calvarial defect after removal of dura. All scale bars = 200 μm; *, $p < .05$.

significantly reduced levels of tHO, consistent with the role of TAK1 in the development of ossification centers. Because tHO forms through an inflammatory stimulus (e.g., trauma), we subsequently focused on genetic loss of *Tak1* only in the mesenchymal cells which contribute directly to the developing ectopic anlagen of tHO using the Prx promoter (Prx-cre) [14]; indeed, we found that in vivo genetic loss of *Tak1* in mesenchymal cells is sufficient to eliminate tHO. Use of the pharmacologic agent NG-25 to inhibit TAK1 confirmed an approach targeting TAK1 to prevent tHO. As expected, in vitro experiments confirmed that genetic loss of Tak1 or treatment with NG-25 reduced chondrogenic differentiation. However, while NG-25 and 5Z-O, another pharmacologic TAK1 inhibitor, reduced mesenchymal cell proliferation in vitro, genetic loss of *Tak1* increased cellular proliferation. These findings may be attributed to off-target effects of TAK1 inhibitors such as NG-25 which also inhibit other kinases including epidermal growth factor receptor and ABL [33]. These findings also indicate that improved TAK1 inhibitors are required to achieve the therapeutic potential, which is highly encouraged by our genetic data.

Initially, we designed the dual-recombinase mouse model to examine whether a single gene could be targeted to knockout and subsequently reactivate the gene of interest. Several previous studies have combined Cre/lox and Flp/Frt technologies to generate dual-inducible mouse models, these have been used to target different genes [33, 34]. Therefore, these technologies have been used to temporally control different genes. The LoxP-FRT Trap (LOFT) method has been reported to disrupt a floxed copy of a gene and subsequently reactivate another copy of the same gene that has been inactivated via gene-trap; however, in that model, gene knockout is caused by Cre-induced removal of the floxed copy with "reactivation" of a second copy of the gene which is silent until treated with Flp. Since gene-trap is used to initially inactivate the second copy, genes applicable for this method need to be expressed in embryonic stem cells, and it may be difficult to predict efficiency of inactivation of the gene trapped allele

that is known to vary gene to gene. There have been no other reports using the LOFT approach, and no reports of a gene knockout/reactivation strategy for tissue regeneration [35].

In this study, we invoke a similar principle of gene inactivation and reactivation using Cre/lox and Flp/Frt technologies but with a simpler and more straightforward targeting strategy (COSIEN technology). Serendipitously, we found that genetic disruption of *Tak1* increases proliferation and reduces differentiation, leading us to wonder whether reactivation of *Tak1* could rescue cellular differentiation after a period of knockout-induced proliferation. The dual recombinase mouse model allowed us to study this, as pharmacologic inhibition of TAK1 with available agents does not increase proliferation. Though an inducible siRNA strategy can be used to silence and reactivate a gene, there are important distinctions between siRNA and our COSIEN technology: (a) the COSIEN technology completely knocks out gene function in a given cell, whereas siRNA has a more limited knockdown, and (b) even though COSIEN recombination efficiency is not perfect, there is a mixture of knockout cells and wild-type cells that is advantageous when cell fate specification is in question and proliferative ability of each cell is in question.

Finally, our findings shed light on the importance of considering the effects of target inhibition and subsequent reactivation in the context of wound healing. Current efforts at tissue regeneration are focused on reducing apoptosis and/or increasing proliferation [2–5]. However, this strategy does not account for the contribution of cellular differentiation and production of noncellular components to tissue regeneration, primarily ECM which is laid down by cells and forms an integral part of tissue morphology. Other strategies which include cell transplantation or scaffold use face hurdles to long-term incorporation and regulatory clearance. Here, we show that an approach including target inhibition and reactivation may allow for a period of proliferation followed by subsequent return of cell differentiation, thereby reconstituting the functional tissue of interest.

Acknowledgments

We thank the University of Michigan Center for Molecular Imaging and Amanda Welton for her assistance. This work was supported, in part. S.A. was funded by NIH F32 AR066499, NIH Loan Repayment Program; S.J.L. and J.D. was funded by Howard Hughes Medical Institute (HHMI) Medical Fellows Program; K.R. was funded by NIH F32 AR068902; Y.M. was funded by NIH R01DE020843, DoD W81XWH-11-2-0073; M.T.L. was funded by California Institute for Regenerative Medicine (CIRM) Clinical Fellow Training grant TG2-01159, American Society of Maxillofacial Surgeons (ASMS)/Maxillofacial Surgeons Foundation (MSF) Research Grant Award, the Hagey Laboratory for Pediatric Regenerative Medicine and e Oak Foundation, NIH grant U01 HL099776, and the Gunn/Olivier Fund; M.I. was funded by the Plastic Surgery Foundation National Endowment Award; B.L. was funded by NIH, NIGMS K08GM109105, NIH R01GM123069, NIH1R01AR071379, American Association of Plastic Surgery Research Fellowship, Plastic Surgery Foundation/AAPS Pilot Research Award, ACS Clowes Award, and International Fibrodysplasia Ossificans Progressiva Association Research Award. Some of this work was supported by Defense Medical Research and Development Program (Clinical and Rehabilitative Medicine Research Program [CRMRP]/ Neuromusculoskeletal Injuries Research Award [NMSIRA]) grant CDMRP: W81XWH-14-2-0010 and Clinical and Rehabilitative Medicine Research Program (CRMRP)/Peer Reviewed Orthopedic Research Program (PRORP): W81XWH-16-2-0051.

Author Contributions

H.H.S.H., S.A., Y.M., B.L.: study design; H.H.S.H., S.A., D.J.C., S.J.L., K.K., A.H., M.T.C., K.R., J.H., J.L., J.N., J.R., A.K., J.D., C.B., C.R.P., C.B., J.P., S.U.O., Y.S.N., S.L., Y.M., B.L.: study conduct, data collection, and data analysis; M.I., G.S., P.H.K., M.T.L., K.W., N.G., J.N.-T., Y.M., B.L.: provide critical materials; H.H.S.H., S.A., D.J.C., M.T.C., S.J.L., Y.M., B.L.: drafting manuscript; H.H.S.H., S.A., D.J.C., S.J.L., K.K., A.H., M.T.C., K.R., J.H., J.L., J.B., J.R., A.K., J.D., C.B., C.R.P., J.N., C.B., J.P., S.U.O., Y.S.N., S.L., M.I., G.S., P. H.K., M.T.L., K.W., N.G., J.N.-T., Y.M., B.L.: approving final version of manuscript; H.H.S.H., S.A., Y.M., B.L.: take responsibility for the integrity of the data analysis.

Disclosure of Potential Conflicts of Interest

B.L. began collaboration with Boehringer Ingleheim after data collection and final submission of this manuscript was complete. N.G. declares employment/patient holder with Dana Farber Cancer Institute; advisory role with Syros, Gatekeeper, Soltego, B2S, Petra, and C4 therapeutics; research funding with Taiho, Astellas, Takeda, Vivid Biosciences, Kinogen, and Aduro; ownership interest with Syros, Gatekeeper, Petra, C4, Soltego, and Aduro. The other authors indicated no potential conflicts of interest.

Data Availability Statement

The datasets generated during and/or analyzed during the current study are available in the GEO Repository, GEO Submission (GSE126118; NCBI tracking system #19738436).

References

1 Levi B, Hyun JS, Montoro DT et al. In vivo directed differentiation of pluripotent stem cells for skeletal regeneration. Proc Natl Acad Sci USA 2012;109:20379–20384.

2 Levi B, Hyun JS, Nelson ER et al. Nonintegrating knockdown and customized scaffold design enhances human adipose-derived stem cells in skeletal repair. Stem Cells 2011;29: 2018–2029.

3 Koria P. Delivery of growth factors for tissue regeneration and wound healing. BioDrugs 2012;26:163–175.

4 Fan F, He Z, Kong LL et al. Pharmacological targeting of kinases MST1 and MST2 augments tissue repair and regeneration. Sci Transl Med 2016;8:352ra108.

5 Peng T, Frank DB, Kadzik RS et al. Hedgehog actively maintains adult lung quiescence and regulates repair and regeneration. Nature 2015;526:578–582.

6 Zhang Y, Desai A, Yang SY et al. Tissue regeneration. Inhibition of the prostaglandin-degrading enzyme 15-PGDH potentiates tissue regeneration. Science 2015;348: aaa2340.

7 Zhang Y, Strehin I, Bedelbaeva K et al. Drug-induced regeneration in adult mice. Sci Transl Med 2015;7:290ra292.

8 Cheng F, Shen Y, Mohanasundaram P et al. Vimentin coordinates fibroblast proliferation and keratinocyte differentiation in wound healing via TGF-beta-Slug signaling. Proc Natl Acad Sci USA 2016;113:E4320–E4327.

9 Dutta P, Sager HB, Stengel KR et al. Myocardial infarction activates CCR2(+) hematopoietic stem and progenitor cells. Cell Stem Cell 2015;16:477–487.

10 Leung Y, Kandyba E, Chen YB et al. Bifunctional ectodermal stem cells around the nail display dual fate homeostasis and adaptive wounding response toward nail regeneration. Proc Natl Acad Sci USA 2014;111: 15114–15119.

11 Velasquez LS, Sutherland LB, Liu Z et al. Activation of MRTF-A-dependent gene expression with a small molecule promotes myofibroblast differentiation and wound healing. Proc Natl Acad Sci USA 2013;110:16850–16855.

12 Zeitouni S, Krause U, Clough BH et al. Human mesenchymal stem cell-derived matrices for enhanced osteoregeneration. Sci Transl Med 2012;4:132ra155.

13 Zhou X, Tan M, Nyati MK et al. Blockage of neddylation modification stimulates tumor sphere formation in vitro and stem cell differentiation and wound healing in vivo. Proc Natl Acad Sci USA 2016;113:E2935–E2944.

14 Agarwal S, Loder S, Brownley C et al. Inhibition of Hif1alpha prevents both trauma-induced and genetic heterotopic ossification. Proc Natl Acad Sci USA 2016;113:E338–E347.

15 Dey D, Bagarova J, Hatsell SJ et al. Two tissue-resident progenitor lineages drive distinct phenotypes of heterotopic ossification. Sci Transl Med 2016;8:366ra163.

16 Hatsell SJ, Idone V, Wolken DM et al. ACVR1R206H receptor mutation causes fibrodysplasia ossificans progressiva by imparting responsiveness to activin A. Sci Transl Med 2015;7:303ra137.

17 Yu PB, Deng DY, Lai CS et al. BMP type I receptor inhibition reduces heterotopic [corrected] ossification. Nat Med 2008;14: 1363–1369.

18 Agarwal S, Sorkin M, Levi B. Heterotopic ossification and hypertrophic scars. Clin Plast Surg 2017;44:749–755.

19 Peterson JR, De La Rosa S, Eboda O et al. Treatment of heterotopic ossification through remote ATP hydrolysis. Sci Transl Med 2014;6: 255ra132.

20 Ranganathan K, Loder S, Agarwal S et al. Heterotopic ossification: Basic-science principles and clinical correlates. J Bone Joint Surg Am 2015;97:1101–1111.

21 Bush JR, Beier F. TGF-beta and osteoarthritis—The good and the bad. Nat Med 2013;19:667–669.

22 Fortier LA, Barker JU, Strauss EJ et al. The role of growth factors in cartilage repair. Clin Orthop Relat Res 2011;469:2706–2715.

23 Greenblatt MB, Shim JH, Glimcher LH. TAK1 mediates BMP signaling in cartilage. Ann N Y Acad Sci 2010;1192:385–390.

24 Gunnell LM, Jonason JH, Loiselle AE et al. TAK1 regulates cartilage and joint development via the MAPK and BMP signaling pathways. J Bone Miner Res 2010;25:1784–1797.

25 Leah E. Osteoarthritis: TGF-beta overload at bones of cartilage degeneration. Nat Rev Rheumatol 2013;9:382.

26 Shim JH, Greenblatt MB, Xie M et al. TAK1 is an essential regulator of BMP signalling in cartilage. EMBO J 2009;28:2028–2041.

27 Zhen G, Wen C, Jia X et al. Inhibition of TGF-beta signaling in mesenchymal stem cells of subchondral bone attenuates osteoarthritis. Nat Med 2013;19:704–712.

28 Zhao T, Ren H, Jia L et al. Inhibition of HIF-1alpha by PX-478 enhances the anti-tumor effect of gemcitabine by inducing immunogenic cell death in pancreatic ductal adenocarcinoma. Oncotarget 2015;6:2250–2262.

29 Mihaly SR, Ninomiya-Tsuji J, Morioka S. TAK1 control of cell death. Cell Death Differ 2014;21:1667–1676.

30 Sato S, Sanjo H, Takeda K et al. Essential function for the kinase TAK1 in innate and adaptive immune responses. Nat Immunol 2005;6:1087–1095.

31 Ninomiya-Tsuji J, Kajino T, Ono K et al. A resorcylic acid lactone, 5Z-7-oxozeaenol, prevents inflammation by inhibiting the catalytic activity of TAK1 MAPK kinase kinase. J Biol Chem 2003;278:18485–18490.

32 Minoda Y, Sakurai H, Kobayashi T et al. An F-box protein, FBXW5, negatively regulates TAK1 MAP3K in the IL-1beta signaling pathway. Biochem Biophys Res Commun 2009; 381:412–417.

33 Moding EJ, Lee CL, Castle KD et al. Atm deletion with dual recombinase technology preferentially radiosensitizes tumor endothelium. J Clin Invest 2014;124:3325–3338.

34 Schonhuber N, Seidler B, Schuck K et al. A next-generation dual-recombinase system for time- and host-specific targeting of pancreatic cancer. Nat Med 2014;20:1340–1347.

35 Chaiyachati BH, Kaundal R, Zhao J et al. LoxP-FRT Trap (LOFT): A simple and flexible system for conventional and reversible gene targeting. BMC Biol 2012;10:96.

36 Levi B, James AW, Xu Y et al. Divergent modulation of adipose-derived stromal cell differentiation by TGF-beta1 based on species of derivation. Plast Reconstr Surg 2010 Aug;126: 412–425.

37 James AW, Levi B, Commons GW et al. Paracrine interaction between adipose-derived stromal cells and cranial suture-derived mesenchymal cells. Plast Reconstr Surg 2010 Sep;126: 806–821.

38 Levi B, Nelson ER, Brown K et al. Differences in osteogenic differentiation of adipose-derived stromal cells from murine, canine, and human sources in vitro and in vivo. Plast Reconstr Surg 2011 Aug;128:373–386.

39 Levi B, Longaker MT. Osteogenic differentiation of adipose-derived stromal cells in mouse and human: in vitro and in vivo methods. J Craniofac Surg, 2011;22:388–391.

See www.StemCells.com for supporting information available online.

11

Noncanonical BMP Signaling Regulates Endochondral Bone Development and Trauma-Induced Heterotopic Ossification

Hsiao Hsin Sung, DDS, Shailesh Agarwal, MD, Shawn Loder, BS, James Drake, BS, David Cholok, BS, John Li, MD, Kavitha Ranganathan, MD, Shuli Li, MD, Yuji Mishina, PhD, Benjamin Levi, MD
From the University of Michigan, Ann Arbor, Mich.

PURPOSE: Canonical bone morphogenetic protein signaling plays a central role in endochondral bone development and trauma-induced heterotopic ossification (HO). However, the role of noncanonical bone morphogenetic protein signaling through the transforming growth factor-activated kinase (TAK1) pathway has not been evaluated in HO. We hypothesize that the TAK1 pathway is crucial for endochondral bone development and HO.

METHODS: Cre-conditional TAK1 knockout mice (*Prx1-Cre;Tak1$^{fl/fl}$) growth plates were evaluated during early postnatal development (P3-P8).* Tamoxifen inducible TAK1 knockout (*Ubi.CreERT*;*Tak1$^{fl/fl}$*) and *Prx1-Cre;Tak1$^{fl/fl}$* mice and *littermate controls* underwent Achilles' tenotomy with 30% TBSA. Micro-computed tomography imaging, histological analysis, osteogenic differentiation and RNA/protein analysis were performed to assess the TAK1 pathway in the cartilaginous HO.

RESULTS: *Ubi.CreERT*;*Tak1$^{fl/fl}$* mice formed 30% less ectopic bone compared with control 9 weeks after burn/tenotomy ($P < 0.05$) (A). *Prx1-Cre;Tak1$^{fl/fl}$* mice exhibit smaller tibia bone size, more immature proliferating chondrocytes, and disorganization of mature bone. Mesenchymal cells isolated from tamoxifen-inducible Tak1 knockout mice showed decreased osteogenic and chondrogenic potential compared with cells from littermates (B and C). In vitro inhibition with TAK1 inhibitor NG-25 similarly significantly reduced chondrogenic and osteogenic differentiation ($P < 0.05$) (D).

CONCLUSIONS: TAK1 plays a prominent role in chondrogenesis during limb development and ectopic bone formation, confirmed by abnormal bone growth and diminished HO in knockout mice. NG-25 appears to be a candidate drug for TAK1 inhibition, which we will evaluate for the treatment of HO using our burn/tenotomy model.

12

Reconstructing Craniofacial Trauma with Fat Grafting: Predictors of Successful Outcomes

Debra Bourne, MD,* Jacqueline Bliley, MS,*† Isaac James, MD,* Gretchen Haas, PhD,‡ Albert D. Donnenberg, PhD,§ Vera Donnenberg, PhD,§ Barton Branstetter, MD,¶ Ryan TM Mitchell, MD,|| Spencer Brown, PhD,** Kacey Marra, PhD,*†§ Sydney Coleman, MD,*†† J Peter Rubin, MD*†§
*From the *University of Pittsburgh Medical Center, Department of Plastic Surgery, Pittsburgh, Pa. †University of Pittsburgh Department of Bioengineering, Pittsburgh, Pa. ‡University of Pittsburgh Medical Center, Department of Psychiatry, and the VA Pittsburgh Healthcare System, Pittsburgh, Pa. §University of Pittsburgh McGowan Institute of Regenerative Medicine, Pittsburgh, Pa. ¶University of Pittsburgh Medical Center, Department of Radiology, Pittsburgh, Pa. ||The Bengtson Center for Aesthetics and Plastic Surgery, Grand Rapids, Mich. **Cooper Medical School of Rowan University, Camden, N.J. ††New York Langone Medical Center, New York, N.Y.*

PURPOSE: Craniofacial disfigurement creates psychological distress and functional impairment. Fat grafting improves contour; however, unpredictability of volume retention is a significant limitation.

METHODS: This institutional review board-approved prospective cohort study was funded by the US Department of Defense. Twenty patients with craniofacial deformities underwent fat grafting. Volume retention was evaluated using computed tomography scans. A portion of fat was evaluated for stromal vascular fraction cell type populations by flow cytometry. Quality of life measures were recorded. Five patients underwent a second fat grafting procedure after completing the 9-month follow-up period.

RESULTS: Volume retention stabilized at 3 months and averaged 63% (±16%) at 9 months. The retention at 3 months was significantly predictive of 9 month volume ($P = 0.006$). Higher stromal vascular fraction cell viability was correlated with improved volume retention ($P = 0.008$). Volume retention in the first procedure was predictive of the second operation ($P = 0.05$). Satisfaction with physical appearance ($P = 0.001$) and social functioning quality of life ($P < 0.04$) improved from baseline to 9 months. There were no serious adverse events.

CONCLUSIONS: Fat grafting craniofacial defects is effective in improving volume deficits, with 40% volume loss anticipated. Viability of fat harvested impacts overall retention. The volume retention in subsequent procedures in the same patient had similar volume retention, suggesting a role for innate biologic characteristics of fat tissue in fat graft healing.

BACKGROUND: Both internal and external distraction devices have been used successfully in correcting midface hypoplasia. Although the indication for surgery and the osteotomy techniques for a Le Fort I and Le Fort III may be similar, deciding when to use an internal vs external device has not been well studied. We studied patient reported outcomes using the FACE Q Patient Reported Outcomes Instrument and functional surveys for internal and external devices for both Le Fort I and Le Fort III patients.

METHODS: Midface hypoplasia patients who underwent distraction advancement after Le Fort I and Le Fort III were surveyed using the FACE-Q survey and a functional survey. Equal groups of internal and external device patients were compared (n=64). Data recorded included: Sex, age, follow-up, diagnosis, OR time, EBL, Length of stay, distraction length, consolidation time, and complications. FACE Q scales included: Satisfaction with Facial Appearance, Social Function (confidence), Psychological Well-being, Early life impact (recovery), and Satisfaction with Outcome and Decision. Functional surveys included Airway/Breathing (correction of sleep apnea, removal of tracheostomy), Ocular/Vision (globes protection), Occlusion/Eating, and Speech/Articulation.

RESULTS: Internal and external device groups were similar with regards to patient demographics (Craniofacial diagnosis, mean age (14.4 years), sex, follow-up), operative time, EBL, distraction length (24.2 vs 25.1), and follow-up. Consolidation times differed (Internal=1.1 vs External=3.6 months). For FACE Q appearance appraisal (Overall Appearance, Cheeks, Nose, Upper lip/Smile), there were similarities in domain and scale. For Functional surveys (Airway/Breathing, Ocular Vision, Occlusion/Eating, Speech/Articulation), there were also similar scoring between groups. However, internal device patients had superior scores compared to external devices with FACE Q for Quality of Life including: Social Function (80.9 ± 19 vs 68.9 ± 18), Early Life Impact (92.9 ± 22 vs 62.4 ± 11), Dental anxiety (70.2 ± 17 vs 48.3 ± 10), and Psychological Well-being (87.8 ± 18 vs 68.6 ± 11). In addition, internal device patients were better with FACE Q Satisfaction Decision (81.2 ± 19 vs 56.9 ± 10) and Satisfaction Outcome (91.0 ± 22 vs 84.7 ± 18).

CONCLUSIONS: Le Fort I and Le Fort III distraction patients had similar patient reported outcomes for appearance and functional improvement while using internal or external devices; however, those with internal devices were more satisfied with their quality of life and decision to undergo the procedure.

123

Loss Of TGF-beta Activated Kinase (TAK1) Activity Induces Cellular Proliferation And Diminishes Differentiation During Bone Healing

Shawn Loder, BS, Shailesh Agarwal, MD, Hsiao Hsieh, Hsung, David Cholok, BS, Michael Chung, MD, John Li, MD, Christopher Breuler, BS, Caitlin Priest, BS, Kavitha Ranganathan, MD, Joseph Habbouche, BS, Arminder Kaura, BS, John Butts, BS, Shuli Li, PhD, Yuji Mishina, PhD, Benjamin Levi, MD

University of Michigan, Ann Arbor, MI

PURPOSE: The ability to modulate signaling pathways at the site of injury represents a novel paradigm in wound healing with implications for regenerative medicine and tissue engineering. Transforming growth factor-beta (TGF-β) activating kinase 1 (TAK1) is a key regulator in the TGF-β and bone morphogenetic protein (BMP) signaling pathways with central roles in proliferation, differentiation, survival, and apoptosis of myriad tissues during development and in a range of pathologic processes. Here we examine the effect of TAK1 inhibition both *in vitro* and in the *in vivo* wound environment. We introduce a novel dual inducible Cre/loxP and Flp/FRT recombinase system to precisely control the expression of TAK1 during wound healing and identify a role for TAK1 as a molecular switch between mesenchymal cell proliferation and differentiation.

METHODS: We developed a novel dual recombinase system (Cre/loxP; Flp/FRT) allowing TAK1 to be specifically inactivated (Ad.Cre) and sequentially re-activated afterwards (Ad.Flp). We first evaluated the effect of this system *in vitro* mesenchymal cells harvested from sites of musculoskeletal injury. Osteogenic differentiation was assayed via alizarin red and alkaline phosphatase staining. SMAD protein signaling was analyzed directly via immunocytochemistry and western blot analysis. Proliferation was assayed directly via BrdU and cell counting. *In vivo, c*ritical sized-calvarial defects (4mm) were performed and mice received either: 1. Ad.LacZ (control) or 2. Ad.Cre (inactivation) or 3. Ten days Ad.Cre (inactivation) followed by Ad.FLP (reactivation) to modulate *Tak1* expression. Calvarial tissue was harvested to assay for gene expression and cellular proliferation and differentiation were quantified histologically.

RESULTS: *In vitro* analysis of mesenchymal cells carrying the Ad.Flp/Ad.Cre construct demonstrated a significant loss in osteogenic potential ($p<0.05$) and pSMAD1/5 signaling in the absence of *Tak1*. Reactivation of *Tak1* was sufficient to restore pSMAD1/5 signaling and osteogenic differentiation. Tak1 knockout demonstrated an opposite effect on cell proliferation with immediate and significant ($p<0.05$) increases in cell growth upon knockout and normalization of cell proliferation on gene reactivation. Loss of *Tak1* in the calvarial wound environment resulted in increased presence of mesenchymal cells and increased expression of proliferative genes including *Ccnd1*, *E2f1*, and *Ki67*, an effect reversed by Ad.Flp reactivation of *Tak1*. Consistent with our *in vitro* data, loss of *Tak1* in calvarial tissue led to diminished osteogenic differentiation genes including *Bmp2*, *Tgfβ1*, *Col1*, *Ocn*, and *Runx2*. Again this effect was reversed by Ad.Flp reactivation of *Tak1*.

CONCLUSION: We demonstrate that precise control of Tak1 can be used to modulate a switch between proliferation and osteogenic differentiation in mesenchymal cells. These findings are possible due to a novel dual-recombinase system with applications in other animal models studying TGF-B signaling and TAK1. Our *in vivo* data suggests that therapeutic modulation of Tak1 may provide a target to control the proliferation/differentiation switch required during tissue regeneration.

124

Using Small Molecule Screens to Identify Novel IRF6 Gene Regulatory Pathways in Orofacial Cleft Pathogenesis

Edward Li, BA, Dawn Truong, BA, Brittany Garrity, BS, Christina Nguyen, BS, Kusumika Mukherjee, PhD, Eric C. Liao, MD-PhD

Massachusetts General Hospital, Boston, MA

PURPOSE: Mutations in the transcription factor *IRF6* represent the most common genetic determinant of both syndromic and nonsyndromic cleft lip and/or palate (CL/P). We hypothesized that the *IRF6* gene regulatory network contains pharmacological targets that could prevent CL/P *in utero*, much like the dramatic effect of prenatal folate supplementation on the incidence of spina bifida. CRISPR genome editing was used to disrupt *irf6* in zebrafish. All mutant embryos displayed an embryonic epithelium (periderm) rupture phenotype, which represents a sensitive platform for high-throughput chemical screening identifying small molecules that could modulate the *irf6* pathways to prevent periderm rupture and potentially CL/P pathogenesis. Using our *irf6* mutant model, here we present a small molecule screen of known bioactives for modulation of Irf6 activity in zebrafish, and identification of molecular pathways that could play a role in palate development.

METHODS: Mutant *irf6-/-* embryos were dispensed 10 embryos per well in 96-well plates and incubated in media containing propidium iodide (renders ruptured embryos fluorescent). The ICCB known-bioactives library containing FDA-approved drugs with well-characterized biological targets was screened. Mutant embryos treated with DMSO were used as solvent controls. Wildtype embryos treated with drugs were used as toxicity controls. Time-lapse images of the wells were captured by automated bright-field and fluorescence microscopy and analyzed with ImageJ. Molecular pathways associated with the positive hits were identified through the library index and analyzed using computational modeling programs.

RESULTS: 65 of the 480 small molecules screened reached statistical significance in delaying periderm rupture compared to DMSO-treated controls without causing developmental delays in wildtype embryos. The molecular targets of the small molecule hits were analyzed by Gene Ontology and revealed not only molecular pathways previously known to play important roles in palate development such as PDGF and FGF, but also novel pathway connections between *IRF6* and the retinoic acid, aryl hydrocarbon, and adenosine pathways among others. Furthermore, when these pathways were aberrantly modulated in wildtype zebrafish embryos, craniofacial defects were observed.

CONCLUSION: Zebrafish *irf6-/-* embryos represent a robust platform for high-throughput small molecule screens to identify modulators of *IRF6* capable of mitigating cleft pathogenesis. The results identified many critical developmental pathways, some of which have been previously reported as essential in palate development while others have not yet been extensively characterized. These pathways could represent unexplored regulatory mechanisms of palate development and novel nodes of pharmacological intervention for orofacial clefting.